

The Element Abundances in Bare Planetary Nebula Central Stars and the Shell Burning in AGB Stars

Klaus Werner

Institut für Astronomie und Astrophysik, Universität Tübingen, Sand 1, D-72076 Tübingen, Germany

werner@astro.uni-tuebingen.de

and

Falk Herwig

Los Alamos National Laboratory, Theoretical Astrophysics Group T-6, MS B227, Los Alamos, NM 87545, U.S.A.

fherwig@lanl.gov

ABSTRACT

We review the observed properties of extremely hot hydrogen-deficient post-AGB stars of spectral type [WC] and PG1159. Their H-deficiency is probably caused by a (very) late helium-shell flash or a AGB final thermal pulse, laying bare interior stellar regions which are usually kept hidden below the hydrogen envelope. Thus, the photospheric element abundances of these stars allow to draw conclusions about details of nuclear burning and mixing processes in the precursor AGB stars. We summarize the state-of-the-art of stellar evolution models which simulate AGB evolution and the occurrence of a late He-shell flash. We compare predicted element abundances to those determined by quantitative spectral analyses performed with advanced non-LTE model atmospheres. A good qualitative and quantitative agreement is found. Future work can contribute to an even more complete picture of the nuclear processes in AGB stars.

Subject headings: stars: AGB and post-AGB — stars: abundances — stars: atmospheres — stars: evolution — stars: interiors — nuclear reactions, nucleosynthesis, abundances

1. Introduction

Post-AGB stars represent a relatively short-lived transition phase between Asymptotic Giant Branch (AGB) stars and white dwarf (WD) stars. All stars with initial masses between 1 and about $8 M_{\odot}$ become H- and He-shell burning AGB stars and end their lives as WDs with a carbon-oxygen core. The model evolution is shown in Fig. 1 for initially $2 M_{\odot}$. More massive Super-AGB stars up to $12 M_{\odot}$ may end as ONeMg WDs. During the hottest phases, post-AGB stars are surrounded by a planetary nebula (PN), ionized material lost by the precursor AGB star. Canonical stellar evolution predicts that throughout all evolutionary phases these stars retain hydrogen-rich envelopes

which, however, can become contaminated by processed material from the interior by dredge-up events occurring in the Red Giant Branch (RGB) and AGB stages. Such an evolution is described by the solid line in Fig. 1.

Already decades ago, the observation of central stars of planetary nebulae (CSPN) exhibiting emission-line spectra which are very similar to those of massive Wolf-Rayet stars with strong helium and carbon emission lines (i.e. spectral type WC) suggested the existence of hydrogen-deficient post-AGB stars (e.g. Heap 1975). Later, the Palomar-Green Survey revealed a new spectral class of H-deficient post-AGB stars, the PG1159 stars, which are dominated by absorption lines of highly ionised He, C, and O (Wesemael et al.

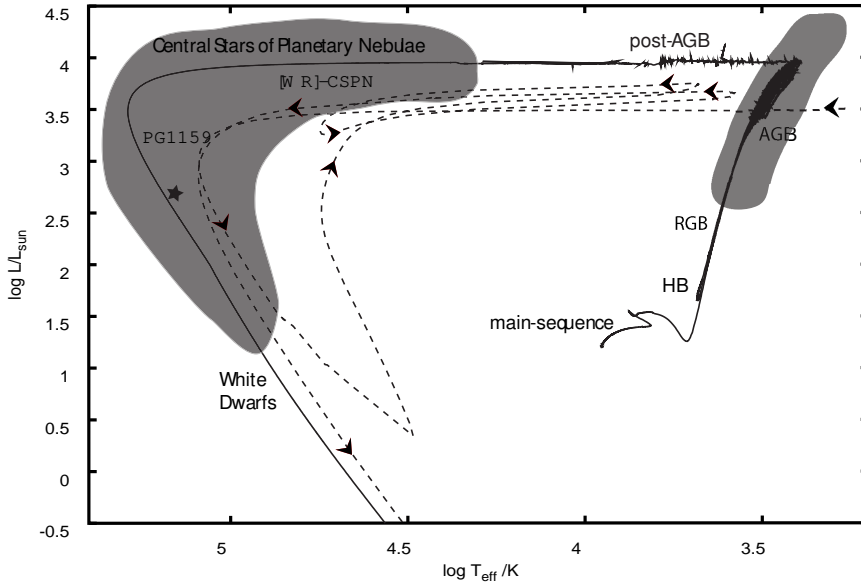


Fig. 1.— Complete stellar evolution track with an initial mass of $2 M_{\odot}$ from the main sequence through the Red Giant Branch phase, the Horizontal Branch phase to the Asymptotic Giant Branch phase, and finally through the post-AGB phase that includes the central stars of planetary nebulae to the final white dwarf stage. The solid line represents the evolution of a H-normal post-AGB star. The dashed line shows a born-again evolution of the same mass, triggered by a very late thermal pulse, however, shifted by approximately $\Delta \log T_{\text{eff}} = -0.2$ and $\Delta \log L/L_{\odot} = -0.5$ for clarity. The star shows the position of PG1159-035.

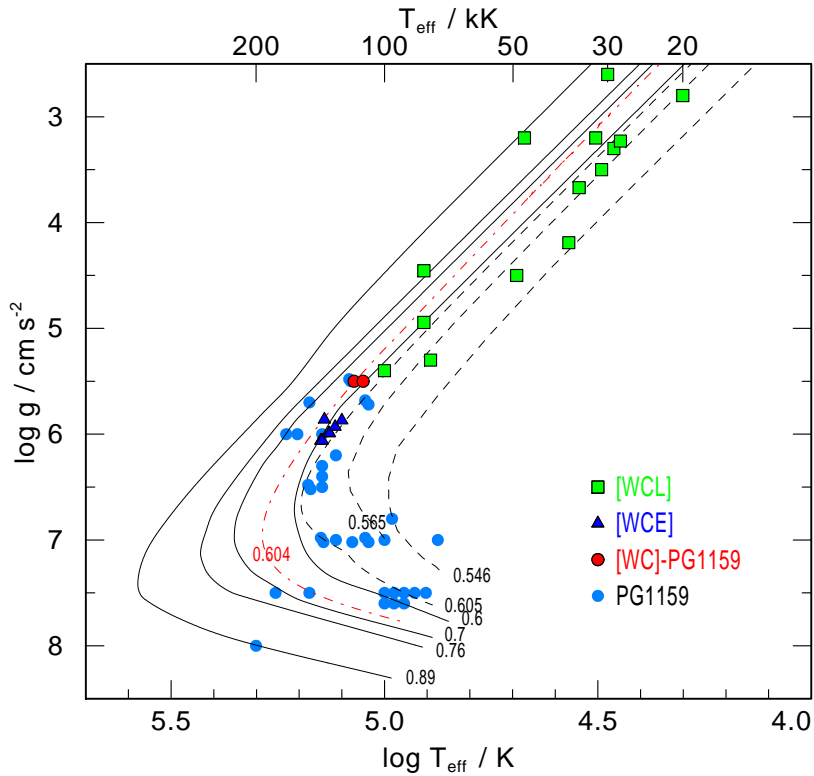


Fig. 2.— Hot hydrogen-deficient post-AGB stars in the g - T_{eff} -plane. We identify Wolf-Rayet central stars of early and late type ([WCE], [WCL], from Hamann 1997), PG1159 stars (from Table 2) as well as two [WC]-PG1159 transition objects (Abell 30 and 78). T_{eff} for the [WC] stars is related to the stellar radius at $\tau_{\text{Ross}}=20$. Evolutionary tracks are from Schönberner (1983) and Blöcker (1995) (dashed lines), Wood & Faulkner (1986) and Herwig (2003) (dot-dashed line) (labels: mass in M_{\odot}). The latter $0.604 M_{\odot}$ track is the final CSPN track following a VLTP evolution and therefore has a H-deficient composition. However, the difference between the tracks is mainly due to the different AGB progenitor evolution.

1985). It is now believed that the PG1159 stars are descendants of the Wolf-Rayet CSPN and that the majority of them will evolve into WDs with helium atmospheres (i.e. non-DA white dwarfs).

The origin of the hydrogen-deficiency in [WC] and PG1159 stars is probably a late helium-shell flash, which means that a post-AGB star (or WD) re-ignites helium-shell burning and transforms the star back into an AGB star. This “born-again AGB star” phenomenon has been discovered in early stellar evolution modeling (Fujimoto 1977; Schönberner 1979) and was later invoked to explain the H-deficiency observed in some hot post-AGB stars (Iben et al. 1983; Herwig et al. 1999). A complete evolutionary track of such a born-again evolution is shown as a dashed line in Fig. 1. The late He-shell flash causes complete envelope mixing. Hydrogen is ingested and burnt and the surface chemistry of the star becomes dominated by the composition of the previous He/C/O-rich intershell layer (the region between the H- and He-burning shells of the AGB star, see Sect. 3.1).

In “usual”, i.e. hydrogen-rich (post-) AGB stars intershell matter can be dredged up to the surface (so-called third dredge-up) and results in the pollution of the photosphere with intershell matter, that is, helium, 3α -burning products (C, O, Ne) as well as s-process elements which are produced by neutron capture in the He-burning environment. The study of s-process element abundances in AGB stars was and is the most important tool to reveal details of the physics of burning and mixing processes. It is essential to understand these processes, because they affect the yields from AGB stars which largely drive the chemical evolution of the Galaxy.

In contrast to these H-rich stars, [WC] and PG1159 stars do not exhibit just traces of intershell matter in their photospheres, but they are essentially made up of intershell matter. This is because the mass of the intershell is much larger than that of the hydrogen envelope and, thus, its composition dominates the mixture of both layers triggered by the late He-flash. These H-deficient post-AGB stars therefore offer the unique possibility to study intershell abundances *directly* and, hence, understand the physical processes leading to the composition.

2. Quantitative spectral analyses

In this section we will summarize results from spectral analyses. We will focus on PG1159 stars (Sect. 2.1) because we think that in particular the abundance analyses for many species is most advanced for this spectral subclass. We will then turn to the [WC] central stars (Sect. 2.2) with emphasis on evidence for the evolutionary link with the PG1159 stars. Both, [WC] and PG1159 stars are thought to result from a late He-shell flash which, however, is still debated. We will later discuss observations that appear to challenge the “born-again” scenario and we will touch upon alternative ideas. In any case, these stars are obviously exhibiting intershell matter and thus are of immediate interest for insight into AGB evolution.

Besides [WC] and PG1159 stars, there exist several other spectroscopic subclasses of H-deficient post-AGB stars which certainly cannot be explained by the “born-again” scenario. These subtypes comprise RCB stars, extreme helium B-stars, helium-rich subdwarf O stars, and the O(He) central stars. They all generally have helium-dominated atmospheres in contrast to [WC] and PG1159 stars which usually have high carbon abundances. These helium-dominated subtypes might form a distinct post-AGB evolutionary channel being caused by a stellar merging event. Because the origin of their abundance patterns is unclear, they are – at the moment – not useful for probing AGB evolution. Therefore we will discuss these subtypes for completeness only (Sect. 2.3), to order the zoo of H-deficient post-AGB stars.

Table 1 gives an overview about typical abundance patterns found among all the discussed spectral subclasses. The [WC] stars are subdivided into late-type and early-type stars, [WCL] and [WCE]. In addition, a [WC]-PG1159 transition type has been introduced, denoting objects with a mixed emission/absorption line spectrum.

2.1. PG1159 stars

2.1.1. Spectral classification

The optical spectra of PG1159 stars are characterized by weak and broad absorption lines of He II and C IV, sometimes with central emission reversals. The hottest objects also display O VI and

TABLE 1

ELEMENT ABUNDANCES (MASS FRACTIONS) IN REPRESENTATIVE HYDROGEN-DEFICIENT POST-AGB STARS OF DIFFERENT SPECTRAL CLASSES. WE DISCUSS TWO POSSIBLE EVOLUTIONARY SEQUENCES: 1. [WCL] \rightarrow [WCE] \rightarrow [WC]-PG1159 \rightarrow PG1159, AND 2. RCB \rightarrow EXTREME HE-B-STARS \rightarrow HE-SDO \rightarrow O(He)

Spectral Class Star	T_{eff} [K]	$\log g$ [cgs]	H	He	C	N	O	F	Ne	Si	S	Fe	note	ref
[WCL]														
IRAS 21282	28 000	3.2	.10	.43	.46	<.005	.01			<.001			H present	2
PM1-188	35 000	3.7	.01	.39	.47	.01	.07		.03	.025			N present, Si high	2
He2-459	77 000	4.4	<.02	.40	.50		.10						typical He/C/O	2
[WCE]														
NGC 1501	134 000	6.0		.50	.35		.15						typical He/C/O	1
Sanduleak 3	140 000	6.0		.62	.26	.005	.12						N present	3
[WC]-PG1159														
Abell 78	115 000	5.5		.33	.50	.02	.15	$1.0 \cdot 10^{-5}$				<.0001	Fe-deficient	4,10,18
PG1159														
HS1517+7403	110 000	7.0		.85	.13	$<3 \cdot 10^{-5}$.02						C,O low	5
HS2324+3944	130 000	6.2	.17	.35	.42	$<.0003^{\text{a}}$.06						H present	11
PG1159-035	140 000	7.0	<.02	.33	.48	.001	.17	$3.2 \cdot 10^{-6}$.02	.00036	.0001	<.0003	typical He/C/O	6,7,9,10,19
PG1144+005	150 000	6.5		.38	.57	.015	.016	$1.0 \cdot 10^{-5}$.02				O low	8,9,10
RCB														
RY Sgr	7 250	0.7	$6 \cdot 10^{-6}$.98	.007	.003	.0009			.00040	.00045	.00020		12
extreme He-B-stars														
BD+10°2179	16 900	2.5	$1 \cdot 10^{-4}$.98	.02	.0008	.0004			.00013	.00007	.00063		13
He-sdO														
BD+37°442	60 000	4.0	<.001	.97	.025	.003				.00079				14
KS292	75 000	5.5	.32	.65	.023	.013								15
O(He)														
K1-27	105 000	6.5	<.05	.98	<.015	.017							N present	16
LoTr4	120 000	5.5	.11	.89	<.010	.003	<.03						H,N present	16
HS1522+6615	140 000	5.5	.02	.97	.01								H,C present	16
Sun														
			.73	.25	.0029	.00089	.0079	$5.0 \cdot 10^{-7}$.0018	.00072	.00050	.0013		17

^auncertain

References. — (1) Koesterke & Hamann (1997); (2) Leuenhagen & Hamann (1998); (3) Koesterke & Hamann (1997); (4) Werner & Koesterke (1992); (5) Dreizler & Heber (1998); (6) Werner et al. (1991); (7) Werner (1996); (8) Werner & Heber (1991); (9) Werner et al. (2004c); (10) Werner et al. (2005); (11) Dreizler (1998); (12) Asplund et al. (2000); (13) Pandey et al. (2005); (14) Bauer & Husfeld (1995); (15) Rauch et al. (1991); (16) Rauch et al. (1998); (17) Grevesse & Sauval (2001); (18) Werner et al. (2003); (19) Jahn (2005)

TABLE 2

THE KNOWN PG1159 STARS AND RESULTS OF SPECTROSCOPIC ANALYSES. IT IS ALSO NOTED IF THE STAR IS A PULSATING VARIABLE OBJECT AND IF IT HAS A PLANETARY NEBULA. OBJECTS WITH DETECTABLE RESIDUAL HYDROGEN ARE DENOTED “HYBRID” STARS.

Star	T_{eff} [1000 K]	$\log g$ [cgs]	C/He ^a	O/He	Mass [M_{\odot}]	Var.	PN	ref. ^b	remark ^c
H 1504+65	200	8.0	>50	>50	0.89	no	no	1	He-deficient
RX J0122.9–7521	180	7.5	0.3	0.17	0.72	no	no	2	
RX J2117.1+3412	170	6.0	1.4	0.16	0.70	yes	yes	3	
HE 1429–1209	160	6.0	1.4	0.16	0.67	yes	no	4	
PG 1520+525	150	7.5	0.9	0.4	0.67	no	yes	3	
PG 1144+005	150	6.5	1.5	0.05	0.60	no	no	3	
Jn 1	150	6.5	1.5	0.8	0.60	no	yes	5	
NGC 246	150	5.7	0.5	0.1	0.72	yes	yes	3	
PG 1159–035	140	7.0	1.5	0.5	0.60	yes	no	3	
NGC 650	140	7.0	?	?	0.60	no	yes	6	:
Abell 21=Ym29	140	6.5	1.5	0.5	0.58	no	yes	2	:
K 1–16	140	6.4	1.5	0.5	0.58	yes	yes	3	:
Longmore 3	140	6.3	1.4	0.16	0.59	no	yes	2	:
PG 1151–029	140	6.0	1.5	0.5	0.60	no	no	2	:
VV 47	130	7.0	1.5	0.4	0.59	no	yes	5	:
HS 2324+3944	130	6.2	1.2	0.16	0.58	yes	no	11	: hybrid
SDSS J102327.41+535258.7	120	7.0	0.9	?	0.58	no	no	7	
Longmore 4	120	5.5	0.9	0.2	0.65	yes	yes	3	
SDSS J001651.42–011329.3	120	5.5	0.6	0.16	0.65		no	7	
PG 1424+535	110	7.0	0.9	0.12	0.57	no	no	3	
HS 1517+7403	110	7.0	0.15	0.02	0.57	no	no	9	
Abell 43	110	5.7	1.2	0.16	0.59	yes	yes	11	: hybrid
NGC 7094	110	5.7	1.2	0.16	0.59	no	yes	11	: hybrid
SDSS J075540.94+400918.0	100	7.6	0.09	?	0.62		no	7	
HS 0444+0453	100	7.5	?	?	0.59		no	8	:
IW 1	100	7.0	?	?	0.56	no	yes	6	:
Sh 2–68	96	6.8	?	?	0.55		yes	10	: hybrid
SDSS J144734.12+572053.1	95	7.6	0.1	?	0.61	no	no	7	
PG 2131+066	95	7.5	0.9	0.4	0.58	yes	no	9	
SDSS J134341.88+670154.5	90	7.6	0.15	?	0.60	no	no	7	
MCT 0130–1937	90	7.5	0.3	0.04	0.60	no	no	2	
PG 1707+427	85	7.5	0.9	0.4	0.59	yes	no	3	
PG 0122+200	80	7.5	0.9	0.4	0.58	yes	no	9	
HS 0704+6153	75	7.0	0.3	0.12	0.51		no	9	
NGC 6852							yes	6	K1–16 type
NGC 6765							yes	6	K1–16 type
Sh 2–78							yes	6	PG 1424+535 type

^aAbundance ratios by mass

^bReference to the most recent spectroscopic work

^cColons denote uncertain, preliminary results of spectroscopic analyses

NOTE.—No spectroscopic analysis of the last three stars was performed. [WC]-PG1159 transition type objects like Abell 78 and Abell 30 are not listed.

References. — (1) Werner et al. (2004a); (2) Werner et al. (2004c); (3) Werner et al. (2005); (4) Werner et al. (2004b); (5) Rauch & Werner (1995); (6) Napiwotzki & Schönberner (1995); (7) Hügelmeyer et al. (2005); (8) Dreizler et al. (1995); (9) Dreizler & Heber (1998); (10) Napiwotzki (1999); (11) Dreizler (1998)

Ne VII lines. Three spectral subclasses have been introduced which allow a coarse characterisation of each star. According to the appearance of particular line features the subtypes “A” (absorption lines), “E” (emission lines), and lgE (low gravity; emission lines) were defined (Werner 1992).

2.1.2. General characteristics: Temperature, gravity and He/C/O abundances; mass-loss rates

First quantitative spectral analyses became feasible with the construction of line blanketed non-LTE model atmospheres accounting for the peculiar chemical composition (Werner et al. 1991). At that time, only a handful of PG1159 stars was identified. Today, 37 PG1159 stars are known. Most of them were found by systematic spectroscopic observations of central stars of old, evolved planetary nebulae (Napiwotzki & Schönberner 1995) as well as follow-up spectroscopy of faint blue stars from various optical sky surveys (Palomar-Green Survey, Montreal-Cambridge-Tololo Survey, Hamburg-Schmidt and Hamburg-ESO Surveys, Sloan Digital Sky Survey) and soft X-ray sources detected in the ROSAT All Sky Survey. In Table 2 we give a complete list of all known PG1159 stars and their location in the $T_{\text{eff}}-\log g$ diagram is shown in Fig. 2. It is seen that they span a wide temperature and gravity range. They represent stars in their hottest phase of post-AGB evolution. Some of them (those with $\log g \lesssim 6.5$) are still helium-shell burners (located before the “knee” in their evolutionary track) while the majority has already entered the WD cooling sequence.

Estimates for mass and luminosity can be obtained by comparison with theoretical evolutionary tracks. The mean mass of PG1159 stars is $0.61 M_{\odot}$ using the older models of H-rich central stars (solid and dashed lines in Fig. 2). However, the H-deficient $0.604 M_{\odot}$ track (dashed-dotted lines in Fig. 2) is systematically hotter than the older tracks, and indicates that the central stars are on average in fact somewhat less massive than that. It is important to note, that the higher temperature of the new tracks is not the result of being H-deficient. Instead, the reason is the more realistic AGB progenitor evolution that now includes the third dredge-up after most of the AGB thermal pulses. This leads to a higher luminosity

for a given core mass and during the post-AGB evolution to higher temperature (Sect. 3.2.4).

Optical spectra are dominated by numerous He II and C IV lines from which the He/C ratio can be derived. Only the hottest objects ($T_{\text{eff}} \gtrsim 120\,000\text{ K}$) exhibit oxygen lines, too, (O VI and, sometimes, very weak O V) so that the O abundance in cooler stars cannot be determined unless UV spectra are available. Similarly, only the hottest objects display optical neon lines (Ne VII) and only UV spectra allow access to the neon abundance in the case of cooler objects. Hydrogen poses a special problem, because all H lines are blended with He II lines. In medium-resolution ($\approx 1\text{ \AA}$) optical spectra hydrogen is only detectable if its abundance is higher than about 0.1 (all abundances in this paper are given in mass fractions). With high-resolution spectra, which are difficult to obtain because of the faintness of most objects, this limit can be pushed down to about 0.02. For PG1159 stars within a PN the situation is even more difficult because of nebular Balmer emission lines.

The He, C, and O abundances show strong variations from star to star, however, a word of caution is appropriate here, too. The quality of the abundance determination is also very different from star to star. For some objects only relatively poor optical spectra were analysed, while others were scrutinized with great care using high S/N high-resolution optical *and* UV/FUV data. Nevertheless, we think that the abundance scatter is real. The prototype PG1159-035 displays what could be called a “mean” abundance pattern: He/C/O=0.33/0.50/0.17. An extreme case, for instance, with low C and O abundances is HS1517+7403, having He/C/O=0.85/0.13/0.02. Taking all analyses into account, the range of mass fractions for these elements is, approximately: He=0.30–0.85, C=0.15–0.60, O=0.02–0.20 (excluding the peculiar object H1504+65, see Sect. 2.1.11). There is a strong preference for a helium abundance in the range 0.3–0.5, independent of the stellar mass (Fig. 3). Only a minority of stars has a higher He abundance, namely in the range 0.6–0.8. There is a tendency that a high O abundance is only found in objects with a high C abundance (Fig. 4).

Some remarks on the possible analysis errors are necessary. As just pointed out, the observa-

tional data are of rather diverse quality, but in general the following estimates hold. The temperature determination is accurate to 10–15%. The surface gravity is uncertain within 0.5 dex. Element abundances should be accurate within a factor of two. The main problem arises from uncertainties in line broadening theory which directly affects the gravity determination and the abundance analysis of He, C, and O.

2.1.3. *Objects with residual hydrogen: Hybrid PG1159 stars*

We already mentioned that hydrogen is difficult to detect. However, four objects clearly show Balmer lines and they are called hybrid PG1159 stars. The deduced H abundance is quite high: $H=0.17$ (Tab. 1, Dreizler 1998). It is worthwhile to note for the discussion on their evolution, that nitrogen is seen in the optical spectra of some of these stars but quantitative analyses are still lacking. The hybrid star NGC 7094 shows Ne and F enhancements like many PG1159 stars (see below). So one can conclude that, aside from the presence of H, the element abundance pattern of the hybrid PG1159 stars seems to resemble that of many other PG1159 stars. However, all the hybrids have not yet been analysed appropriately although good UV and optical spectra are available.

2.1.4. *Nitrogen and pulsation instability*

Some PG1159 stars do show nitrogen lines while others, with similar temperature and gravity, do not. These are N V lines in the optical wavelength range and the resonance line doublet in the UV at 1239/1243 Å. The derived N abundance is of the order 0.01 (Werner & Heber 1991; Dreizler & Heber 1998). The presence of N shows no clear correlation to the relative abundances of the main atmospheric constituents (He, C, O). But a remarkable correlation between the presence of N and the pulsational instability of PG1159 stars has been found: All four pulsating objects in a sample of nine examined PG1159 stars are showing nitrogen (Dreizler & Heber 1998). Among these objects is the prototype PG1159-035, for which we have recently taken a high-resolution HST/STIS spectrum, allowing to separate the interstellar and photospheric components of the N V resonance doublet. As a consequence, we find that the N

abundance is distinctly lower, namely 0.001 (Jahn 2005; Reiff et al. 2005, 2006, and Reiff et al. in prep.), which weakens the nitrogen/pulsation correlation. In any case, such a correlation is difficult to explain with current stellar pulsation models (e.g. Quirion et al. 2004). Due to its low abundance, nitrogen cannot affect pulsational properties, but it was speculated that N is a marker for different evolutionary histories leading to different He/C/O abundances in the pulsation driving regions. More about PG1159 pulsators follows in Sect. 2.1.13.

2.1.5. *Neon*

Neon has been detected in ten PG1159 stars by the identification of Ne VII lines in optical and FUV spectra (Werner & Rauch 1994; Werner et al. 2004c). The derived abundances are of the order 0.02, i.e. roughly ten times solar. Only the hottest and most luminous objects are able to ionize neon strongly enough to show these lines. Unfortunately, no lines from lower ionization stages are observed, so that the neon abundance in cooler PG1159 stars remains unknown. The strongest Ne VII line is found in FUSE spectra, located at 973Å. The absorption line core almost reaches zero intensity in some objects. In the most luminous objects (e.g. K1–16) this line displays a powerful P Cygni profile (Herald et al. 2005).

2.1.6. *Fluorine*

Lines from F V and F VI have been discovered in FUSE spectra of several PG1159 stars (Werner et al. 2005). The derived abundances show a surprisingly strong variation from star to star, ranging between solar and 250 times solar. Correlations between the F and other element abundances are not obvious. We have speculated that the variety of F abundances is a consequence of the stellar mass, which according to Lugaro et al. (2004) strongly affects the production of fluorine.

2.1.7. *Other light metals: Si, P, S*

Lines from silicon, phosphorus, and sulfur were discovered in FUSE spectra of several PG1159 stars. Analyses are currently performed and we can report preliminary results only (Jahn 2005; Reiff et al. 2005, 2006, and Reiff et al. in prep.).

The silicon abundance in PG1159 stars is of interest, because a strong overabundance (up to $\text{Si}=0.03$, i.e. 40 times solar) has been found in a handful of [WCL] stars (Leuenhagen & Hamann 1998). The photospheric component of the Si IV 1394/1402 Å resonance doublet has been identified in the above mentioned HST/STIS high resolution spectrum of the prototype. Our best line fit is obtained with $\text{Si}=0.5$ solar, which means no significant deviation from the solar abundance within error limits. Another silicon line pair, Si IV 1122/1128 Å, can be identified in relatively cool objects only. For PG1424+535 we find a solar silicon abundance from these lines and an upper limit of 0.1 solar for PG1520+525.

Phosphorus was discovered in a number of PG1159 stars by the identification of the P V resonance doublet at 1118/1128 Å. First results for two objects indicate a roughly solar abundance.

The most prominent sulfur feature is the S VI 933/945 Å resonance doublet. It was first detected in K1-16 and a solar S abundance was derived (Miksa et al. 2002). It is also visible in other PG1159 stars. In the prototype star and two other objects we find a surprisingly strong S depletion (less than 0.1 solar).

2.1.8. Iron deficiency

Model spectra for PG1159 stars predict detectable lines from Fe VI and Fe VII in the UV for objects which are not too hot ($T_{\text{eff}} \leq 140000$ K), otherwise iron is ionised to even higher stages which have lines only in the EUV range beyond the Lyman edge. But iron lines are narrow and require high-resolution (≈ 0.1 Å) high-S/N spectra for a quantitative analysis. Up to now, iron has not been detected in *any* PG1159 star. In most cases, a solar Fe abundance cannot be excluded, because the data quality does not allow more stringent conclusions. For two PG1159 stars, however, it was shown that the lack of iron lines means that the iron abundance is subsolar by at least one dex (K1-16 and NGC 7094; Miksa et al. 2002). A similar result was obtained for the [WC]-PG1159 transition object Abell 78 (Werner et al. 2003) and several [WC] stars (see below). The prototype PG1159-035 is subsolar in Fe by at least a factor of five (Jahn 2005). The suggestion of Herwig et al. (2003b) that iron has been transformed into heavier elements will be discussed below. Our

search for lines from elements heavier than Fe has so far been unsuccessful.

2.1.9. Unidentified lines

About two dozen of absorption lines in the 1000–1700 Å region of PG1159 stellar spectra taken with FUSE, HST, and IUE remain unidentified. Most of them are commonly seen in at least two objects, and many are quite prominent. For example, one of the strongest unidentified absorption lines in the UV spectrum of the prototype as well as of other PG1159 stars is located at 1270.2 Å. It always appears together with a small number of weaker absorption lines in the 1264–1270 Å range. It could be a hitherto unidentified neon or magnesium multiplet.

Also, a number of weak lines in high-quality optical spectra remain unidentified, too. We have recently identified one of these features as a Ne VII multiplet, whose wavelength was only inaccurately known before (Werner et al. 2004c).

We are confident that all the unidentified lines do not stem from C or O. It is obvious on the other hand that line lists from other highly ionized metals are rather incomplete, inaccurate or even non-existent. Some of the unidentified lines might stem from other light metals (Mg, Al) or even from heavy metals beyond the iron group, e.g., s-process enhanced elements. We should make every effort to identify these lines. New species could be found and their abundances checked against evolutionary models.

2.1.10. Mass loss; occurrence of ultra-high ionisation lines

PG1159 stars do not exhibit wind features in their optical spectra. UV spectroscopy, however, reveals that many of the low-gravity central stars display strong P Cygni profiles, e.g. of the resonance lines from C IV and O VI; and of subordinate lines from He II, O V, and Ne VII. Mass-loss rates in the range $\log(\dot{M}/M_{\odot}\text{yr}^{-1}) = -8.3 \dots -6.9$ were derived (Koesterke & Werner 1998; Koesterke et al. 1998; Herald et al. 2005) and it appears that they are in accordance with predictions from radiation driven wind theory.

The central star of Longmore 4 showed a remarkable event, turning its spectral type from PG1159 to [WCE] and back again to PG1159,

most probably due to a transient but significant increase of the mass-loss rate (Werner et al. 1992). The reason is unknown but might be connected to the fact that the star is a pulsator. This phenomenon has never been witnessed again, neither in Longmore 4 nor any other PG1159 star. The outburst phenomenon observed in the [WR] central star of the LMC planetary nebula N66 is probably the consequence of mass-transfer within a close-binary system (see Sect. 2.2.4).

The most luminous PG1159 stars display ultrahigh-ionisation *emission* lines, the most prominent one is O VIII 6068 Å (e.g. Werner et al. 1994). This phenomenon is also seen in [WCE] stars and in [WC]–PG1159 transition objects, as well as in the hottest known DO white dwarf (KPD0005+5106). It is clear that the photospheric temperatures are not high enough to produce these lines and it is possible that they arise from shock-heated regions in the stellar wind.

A large fraction of all DO white dwarfs shows such ultrahigh-ionisation lines in *absorption* (e.g. C VI, N VII, O VIII, Ne X, Werner et al. 1995). This remarkable and still unexplained phenomenon was recently discovered for the first time in a new PG1159 star (Hügelmeier et al. 2006). In addition, the usual photospheric absorption lines (He II, C IV) are much stronger than predicted from any model and this behavior, too, is shared with that of the respective DO white dwarfs.

We remark that, even more strange, too-deep photospheric He II absorption lines are exhibited by some DO white dwarfs which do *not* show ultrahigh-ionisation absorption lines at the same time (e.g. Werner et al. 2004b). A respective PG1159-type counterpart has also been discovered (Nagel et al. 2006).

2.1.11. *Peculiar: H1504+65*

H1504+65 displays an optical spectrum that is at first sight rather similar to other hot high-gravity PG1159 stars. However, it has been shown that this object is helium-deficient and its atmosphere is mainly composed of C and O. Probably it has an evolutionary history that is different from all the other PG1159 stars, hence, we will not further discuss this interesting peculiar object (see Werner et al. 2004a, for details).

2.1.12. *Descendants: DA and non-DA white dwarfs*

The coolest high-gravity PG1159 star has $T_{\text{eff}}=75\,000$ K and the hottest white dwarfs have $T_{\text{eff}}\approx 120\,000$ K. In this temperature range the PG1159 stars must be turned into a DA or non-DA white dwarf by gravitational settling, depending on the presence of residual hydrogen in the PG1159 stellar envelope. It is tempting to assume that the majority of the PG1159 stars will become DO and then DB and DQ white dwarfs, but it is unknown to which extent this is true. Clearly, the hybrid-PG1159 stars will become DA white dwarfs, but this could in principle also hold for all other PG1159 stars because a H abundance as high as 0.01 cannot be excluded by spectroscopic means. Depending on the amount of residual H in the PG1159 envelope, DAs with different hydrogen layer mass will emerge. It can be speculated that the ZZ Ceti stars (DA pulsators) for which thin H envelopes were inferred are descendants of PG1159 stars (Althaus et al. 2005a).

2.1.13. *Results from asteroseismology*

Some of the PG1159 stars are non-radial g-mode pulsators (see Tab. 2) and they define the GW Vir (=PG1159-035) instability strip in the HRD (Fig. 5). These variables are among the best studied by asteroseismologic analyses. Such investigations on the interior of PG1159 stars hold important clues for their origin.

In Tab. 3 we summarize the results from asteroseismology of five PG1159 stars plus one [WCE] central star. The agreement between pulsational and spectroscopic mass determinations is very good (within 5%) except for RX J2117.1+3412, where the difference is of the order 20%. This is significant because in order to shift its position in the $\log g - T_{\text{eff}}$ diagram onto the $M_{\text{puls}}=0.56 M_{\odot}$ track, T_{eff} would need to be decreased from 170 000 K to <120 000 K, which is clearly ruled out by detailed optical and UV/FUV spectroscopy. The mass discrepancy is possibly due to inadequate pulsation models, a weakness in their asteroseismic analyses pointed out by Vauclair et al. (2002).

Of considerable interest for comparison with evolutionary calculations is the analysis of the mode-trapping features in the period spacings

TABLE 3

RESULTS FROM ASTEROSEISMOLOGY OF PG1159 STARS AND THE [WC4] CENTRAL STAR OF NGC 1501. WE COMPARE THE STELLAR MASS DERIVED BY SPECTROSCOPIC MEANS M_{spec} (FROM TAB. 2) WITH THE PULSATIONAL MASS M_{puls} . OTHER COLUMNS LIST ENVELOPE MASS M_{env} (ALL MASSES IN SOLAR UNITS) AND ROTATION PERIOD P_{rot} IN DAYS.

Star	M_{spec}	M_{puls}	M_{env}	P_{rot}	ref
PG 2131+066	0.58	0.61	0.006	0.21	1
PG 0122+200	0.58	0.59		1.66	2
RX J2117.1+3412	0.70	0.56	0.045	1.16	3
PG 1159-035	0.60	0.59	0.004	1.38	4
PG 1707+427	0.59	0.57			5
NGC 1501		0.55		1.17	6

References. — (1) Kawaler et al. (1995); (2) Fu & Vauclair (2006); (3) Vauclair et al. (2002); (4) Kawaler & Bradley (1994); (5) Kawaler et al. (2004); (6) Bond et al. (1996)

which allows to investigate the stellar interior structure. Tab. 3 lists the results obtained for the stellar envelope mass M_{env} , i.e. the mass above the chemical discontinuity between the He-rich envelope and the C/O core. These envelope masses are much smaller than the intershell region remaining on top of the C/O core ($M=2 \cdot 10^{-2} M_{\odot}$) immediately after a (very) late thermal pulse. Observational mass-loss determination for FG Sge by Gehrz et al. (2005) show that born-again stars have high mass-loss rates over prolonged periods of time (see Sect. 2.4). These may remove enough mass to indeed identify the envelope mass from pulsation analyses with the mass between the He-free core and the surface. Note, however, that recent investigations involving complete evolutionary models come to the conclusion that the mode-trapping features could result from structures in the C/O core (Córscico & Althaus 2005).

Recent theoretical pulsation driving modeling could clarify important problems. Early stability calculations (e.g. Starrfield et al. 1983) suggested that the C/O κ -mechanism in PG1159 stars is suffering from the so-called H and He poisoning phenomenon. Accordingly, the He abundance in the photospheres, and particularly the H abundance in the hybrid-PG1159 stars, is too high to drive pulsations in the sub-photospheric layers, hence, abundance gradients had to be invoked. It is however difficult to explain how such an abundance gradient could be maintained. The κ -mechanism operates at depths where $T \approx$

10^6 K, which lies in the outer $\approx 10^{-8} M_{\star}$ mass fraction of the star (e.g., Quirion et al. 2004). In the case of RX J2117.1+3412, for instance, the observed mass-loss rate of $\log(\dot{M}/M_{\odot}\text{yr}^{-1}) = -7.4$ (Koesterke & Werner 1998) implies that the material in the driving region is appearing on the surface and renewed on a very short time scale, namely three months. New pulsation modeling with improved opacity tables has shown that this poisoning problem is not so severe and, hence, no abundance gradients need to be invoked (Saio 1996; Gautschy 1997; Gautschy et al. 2005; Quirion et al. 2004). They can even explain the presence of pulsations in the H-rich hybrid-PG1159 stars (Quirion et al. 2005a). However, these results are still at odds with similar calculations performed by others (Cox 2003).

The co-existence of pulsators and non-pulsators in the instability strip can be explained in terms of differences in the chemical surface composition. The red edge of the strip is essentially identical with the location of the coolest high-gravity PG1159 stars. Gravitational diffusion of C and O out of the remaining He-envelope removes the driving agents and turns the PG1159 star into a DO white dwarf (Quirion et al. 2005b). There is no sharp blue edge of the strip, as its position is different for each star, depending on its chemical composition. Asteroseismic analyses of DB white dwarfs confirm the diffusion scenario and the PG1159-DO-DB evolutionary link (Metcalfe et al. 2005).

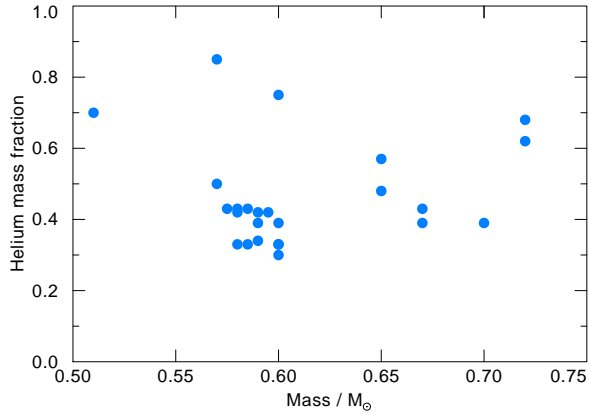


Fig. 3.— Helium mass fraction in PG1159 stars as a function of stellar mass.

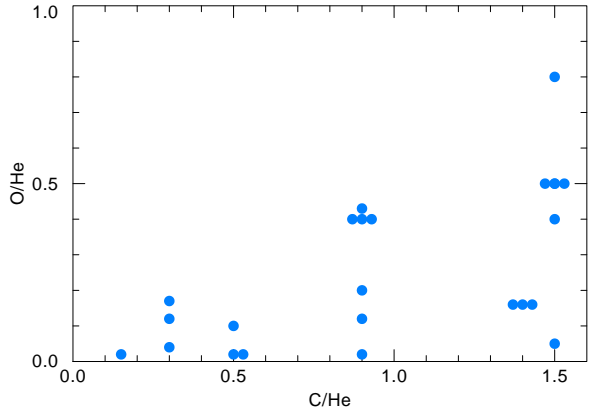


Fig. 4.— Carbon and oxygen abundance ratios relative to helium (by mass) in PG1159 stars.

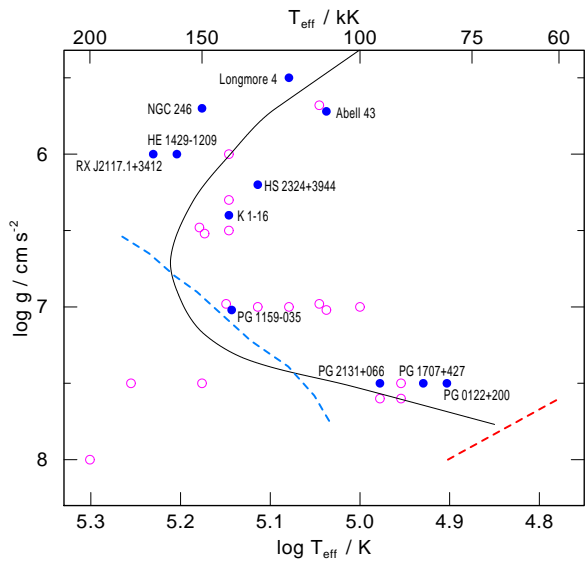


Fig. 5.— The pulsating PG1159 stars (filled symbols with name-tags) and the non-pulsators. The dashed lines are theoretical blue and red edges of the instability strip from Gautschi et al. (2005) and Quirion et al. (2004), respectively. See text for discussion about these edges and the co-existence of non-pulsators in the strip (Sect. 2.1.13). Also shown is the $0.6 M_{\odot}$ post-AGB track from Fig. 2.

2.2. [WC] central stars

[WC] central stars exhibit spectra that are very similar to their massive counterparts. As a consequence of the higher mass-loss rates ($\log(\dot{M}/M_{\odot}\text{yr}^{-1}) = -7.0 \dots -4.9$, Koesterke 2001) compared to PG1159 stars, they show essentially pure emission line spectra, mainly presenting broad and bright lines of He, C, and O.

Recent summaries of [WC] identifications and spectral analyses can be found in Acker & Neiner (2003) and Hamann (2003), respectively.

2.2.1. Abundances in [WC] stars compared to PG1159 stars

The [WC] stars are divided into two subgroups, namely late-type and early-type objects: [WCL] and [WCE]. From their location in the $\log g - T_{\text{eff}}$ diagram (Fig. 2) it is suggestive that they form an evolutionary sequence, but this is at odds with the current state of quantitative spectral analyses. The mean carbon abundance in [WCL] stars is 0.50 while it is lower by about a factor of two in the [WCE]s (Koesterke 2001). In recent re-analyses with new models this difference does not disappear (Hamann et al. 2005). It is conceivable that systematic errors occur because the abundance analyses rely on different spectral lines in [WCL]s and [WCE]s.

Aside from this discrepancy it seems obvious that the PG1159 stars are the progeny of [WC] stars, because they can accommodate the variety of He/C abundance ratios observed in the [WC]s. To corroborate this evolutionary link it is useful to compare other element abundances. We refer to work already quoted in this section and to Leuenhagen & Hamann (1998).

Hydrogen: In three [WCL] stars H was detected and the abundances range between 0.1 and 0.01, however, it has been questioned that the Balmer lines are of photospheric origin (De Marco & Barlow 2001). No H was detected in [WCE] stars, but no strict upper limits can be given ($H \lesssim 0.1$). This is in line with upper limits of about 0.1 for the H abundance in PG1159 stars and the H abundance of 0.17 in the hybrid-PG1159 stars.

Nitrogen: Some [WCL] stars exhibit N lines and abundances of the order 0.01 were found. Also, some [WCE] show N lines and the derived abundances are just slightly lower, namely 0.003–0.005.

These abundances are very similar to those determined for objects in the PG1159 group.

Oxygen: The range of O abundances observed in [WC]s is very similar to that of the PG1159 stars.

Neon: Ne I lines were detected in four [WCL] stars and abundances of the order 0.03 were derived. Again, this is very similar to the PG1159 group.

Silicon: As already mentioned above (Sect. 2.1.7), strong Si overabundances in some [WCL] stars were found, which is at odds with the approximately solar Si abundance we find in the PG1159 prototype. More analyses are needed to see if there exists a large abundance scatter within the [WCE] or PG1159 stars.

Iron: Like in the case of the PG1159 stars, the Fe abundance in [WC] stars has been examined in a few cases only. An iron deficiency has been found, being in qualitative agreement with PG1159 stars. Gräfener et al. (2003) report a low Fe abundance in SMP 61, a [WCE] star in the LMC. Its abundance is at least 0.7 dex below the LMC metallicity. Crowther et al. (1998) find evidence for an underabundance of 0.3–0.7 dex in the Galactic [WCL] stars NGC 40 and BD+30°3639.

2.2.2. [WC]–PG1159 transition objects; weak emission line stars (WELS)

The [WC]–PG1159 class comprises stars which show both, spectral characteristics of PG1159 stars and [WC] stars, namely mixed absorption/emission line spectra. Only two objects can be safely assigned to this group (Abell 30, Abell 78). They have He/C/N/O abundances similar to PG1159 and [WC] stars (Werner & Koesterke 1992).

It must be emphasized that the class of so-called “weak emission line stars” (WELS), which comprises dozens of central stars (e.g. Tylanda et al. 1993), is *not* identical with the [WC]–PG1159 class. The WELS are poorly studied quantitatively, and some of them are clearly “usual” hydrogen-rich post-AGB stars (Méndez 1991; Fogel et al. 2003).

2.2.3. [WO] and O VI classifications

The term “O VI sequence” was coined by Smith & Aller (1969) to denote central stars with the

most highly excited optical stellar spectra. The distinguishing feature of this group is the presence of the O VI 3811/3834 Å emission doublet. In today’s terminology, the O VI stars is a collective name for the hottest [WCE] and PG1159 stars and the [WC]–PG1159 transition objects, which all show O VI emission lines.

The WO class (O for oxygen) was first introduced by Barlow & Hummer (1982) for WR stars with highest excitation spectra. It was also introduced in refined classification systems that are applicable to both, massive WR stars and WR central stars (Crowther et al. 1998; Acker & Neiner 2003). Like in the “O VI sequence” such spectra are exhibited by the hottest objects showing O VI emission lines. In essence, the [WO] classification (with subclasses [WO1] to [WO4]) is used alternatively for the earliest [WCE] subtypes [WC2] and [WC3].

2.2.4. *Are there [WN] central stars?*

It is believed that there are two central stars that exhibit a spectrum similar to massive WN stars, i.e., it is dominated by N instead of C emission lines. For one of these objects (PM5) it cannot be completely ruled out that it is in fact a massive WN star with a ring nebula (Morgan et al. 2003). The other object is the LMC planetary nebula N66. It is thought that this object is a white dwarf accreting matter from a close companion (Hamann et al. 2003) and, hence, its surface composition is not the result of single-star evolution.

2.3. **He-dominated post-AGB objects: RCB, extreme He-B, He-sdO, and O(He) stars**

There exists a small group of four extremely hot objects ($T_{\text{eff}} > 100\,000$ K) which have almost pure He II absorption line spectra in the optical. As introduced by Méndez (1991), these stars are classified as O(He). Their atmospheres are indeed helium dominated, only trace amounts of CNO elements are detected (Rauch et al. 1998, see also Tab. 1 for atmospheric parameters). In the $\log g - T_{\text{eff}}$ diagram they are found among the PG1159 stars. While the born-again evolutionary models can explain the rich diversity of different He/C/O patterns in [WC] and PG1159 stars,

they never result in such helium-dominated surface abundances. It is therefore natural to speculate on the existence of a third post-AGB evolutionary sequence and its origin. The O(He) stars could be the long-searched progeny of the RCB stars, which are relatively cool ($T_{\text{eff}} < 10\,000$ K) stars with helium-dominated atmospheres, too. The so-called “extreme He-B-stars” and the “He-sdO” (post-AGB) stars are also He-dominated and could represent objects in transition phases between RCB and O(He); see Tab. 1 for parameters of some representatives.

The evolutionary link between these He-dominated post-AGB objects still needs to be investigated. They are possibly the result of a merging process of two white dwarfs (e.g. Saio & Jeffery 2002) and, hence, these objects are not of immediate interest to this review.

2.4. **Historical (very) late He-shell flashers**

Three stars have been identified as actual born-again stars, mainly through their historical variability. These are FG Sge (Gonzalez et al. 1998), V605 Aql (Clayton & De Marco 1997) and V4334 Sgr (Sakurai’s object, Duerbeck & Benetti 1996).

For each of these cases an important question is whether the born-again evolution is following a very late thermal pulse (VLTP) or just a late thermal pulse (LTP). As we will discuss in Sections 3.2.1 and 3.2.3 the difference between the two is that the VLTP happens late during the post-AGB evolution, and induces a H-ingestion flash that consumes H in the surface layer by nuclear burning. As recent evolution calculations show (Sect. 3.2.1), the VLTP born-again star follows a characteristic double loop in the HRD, where the first return to the AGB proceeds fast in only a few years, whereas the second return takes much longer, of the order 10^2 yr. The LTP happens earlier, on the horizontal, constant luminosity part of the post-AGB track, and H-deficiency is only the result of dredge-up mixing when the star returns to the AGB. The LTP born-again star follows a single loop on a long time scale, similar to the second return of a VLTP born-again star.

V605 Aql has experienced a VLTP in 1917 (Lechner & Kimeswenger 2004). As summarized in Clayton & De Marco (1997, see more references there) it brightened over a period of only

two years, followed by three episodes of fading and brightening. Then V605 Aql disappeared, enshrouded in its own dust. In the early 1970s its position was found to coincide with that of the planetary nebula Abell 58. It was later discovered that the PN in fact has a small high-velocity, H-deficient central knot, while the outer nebula is H-normal. Spectra taken in 1986 by Seitter (1987a,b) reveal a broad stellar C IV emission line indicative for a very hot ($T_{\text{eff}} \approx 100\,000$ K) [WC] central star, implying that V605 Aql had already started to reheat and became a hot H-deficient or H-free central star. A recent model atmosphere analysis of a VLT spectrum taken in 2002 confirms that V605 Aql is now a [WCE] star, having $T_{\text{eff}} = 95\,000$ K (Fedrow et al. 2005).

For FG Sge it is not so obvious whether it is a LTP or a VLTP born-again star. Lawlor & MacDonald (2003) proposed that while Sakurai's object and V605 Aql are fast evolving VLTP first-return born-again objects, FG Sge has experienced a VLTP too, but it is now on the second, long time-scale return. However, as summarized by Gonzalez et al. (1998, see more references there), FG Sge started to brighten in 1894 until the mid-1970s. Since then the brightness has not changed. FG Sge had initially (in the 1960s) solar abundance. Later (in the 1970s), rare earth elements appeared on the surface, and in 1992 the star underwent dramatic photometric variations due to dust condensation. In the 1990s the carbon and heavy element abundance has further increased, and there is now evidence for H-deficiency. The fact that FG Sge had solar abundances 40 years ago, and only rather recently has shown evidence for H-deficiency is a clear indication that FG Sge is a LTP star as pointed out by Gonzalez et al. (1998). A VLTP born-again star during the second loop should have been already extremely H-deficient, or likely even H-free during the entire past observed evolution, which is not the case. We note, however, that it has been questioned if FG Sge has really become H-deficient (Schönberner & Jeffery 2002).

Sakurai's object is the most recently discovered born-again star (Duerbeck et al. 1997; Duerbeck et al. 2000). Its VLTP has been dated semiempirically between 1992 and 1994, and its T_{eff} dropped below 10 000 K during early 1996. At this time the star was already H-poor, and continued to change

the surface abundance distribution over a period of six months, covered by observations of Asplund et al. (1999). While the H-abundance was decreasing even further, the already high Li abundance continued to increase. In addition, these observations showed the C, N and O abundances to be enhanced significantly compared to solar, as well as a low $^{12}\text{C}/^{13}\text{C}$ and a low Fe/Ni ratio. Since these observations Sakurai's object has shared the fate of the other born-again objects and faded away behind thick clouds of dust. Recent radio observations show that Sakurai's object has already started to reheat (Hajduk et al. 2005), and it too will eventually become a hot H-free or H-deficient central star.

The observations of born-again stars have revealed important information about the mass loss of these objects. Hajduk et al. (2005) find a mass loss rate between 10^{-5} and maybe up to $2 \cdot 10^{-4} M_{\odot}/\text{yr}$ for Sakurai's object during the coolest evolution phase. For FG Sge Gehrz et al. (2005) determined a mass-loss rate of $2.3 \cdot 10^{-5}$ to $1.2 \cdot 10^{-4} M_{\odot}/\text{yr}$.

3. Stellar evolution origin

The abundance pattern observed in H-deficient bare stellar cores can be understood in terms of the evolutionary origin of these stars. The H- and He-burning shells of AGB stars are the nucleosynthetic origin of the material that is observed at the surface of PG1159 and [WC]-CSPN. In order to make this connection plausible we review in this section first those aspects of AGB evolution and nucleosynthesis that are relevant for our purpose, followed by a summary of the current understanding of the born-again evolution that leads to almost complete H-depletion. In Sect. 3.3 we describe the surface abundance predictions of H-deficient post-AGB stars.

3.1. AGB evolution

The basic properties of AGB stars are covered in Iben & Renzini (1983), AGB properties specifically in view of the post-AGB evolution leading to H-deficient cores have been summarized by Bloeker (2001), while an extensive review of more recent developments has been provided by Herwig (2005). AGB stars have an electron-degenerate C/O core as a result of core He-burning. Their nu-

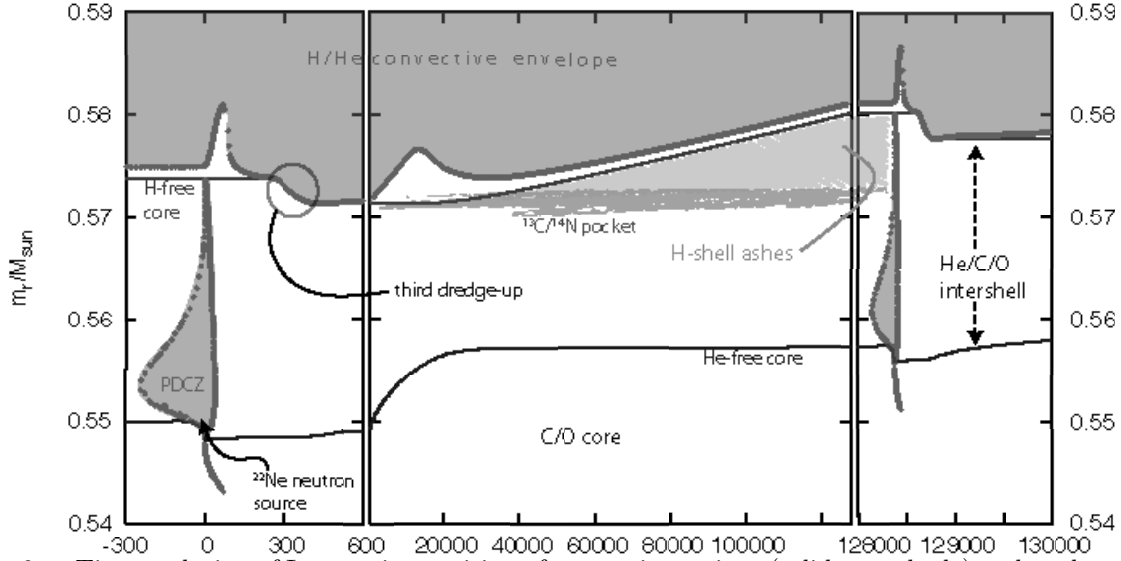


Fig. 6.— Time evolution of Lagrangian position of convective regions (solid grey shade) and nuclear burning shells (at the location of the H- and He-free cores, respectively). The shown time interval comprises one pulse-cycle. Each dot along the boundaries of convective regions corresponds to one time step in the model sequence.

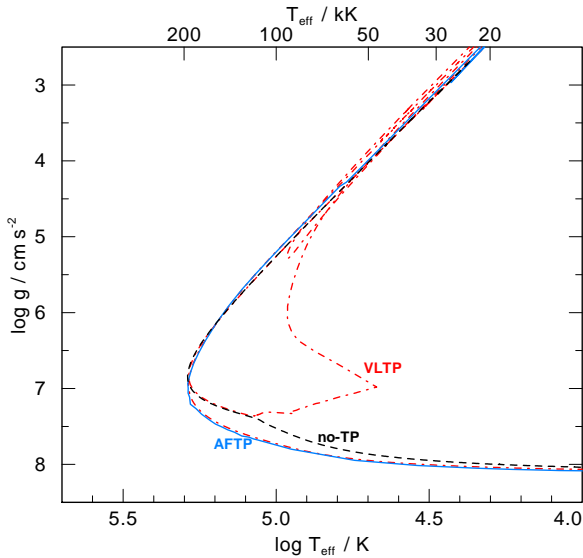


Fig. 7.— Comparison of three different evolution channels in the g - T_{eff} -plane for a $0.604 M_{\odot}$ post-AGB star that had a main sequence mass of $2 M_{\odot}$ and evolved through about a dozen thermal pulses with dredge-up.

clear sources are the He- and the H-burning shells, that surround the core. Double-shell burning on degenerate cores is unstable, and fundamentally similar to the X-ray bursts on the surface of neutron stars. AGB stars experience quasi-periodic bursts of the He-shell. These He-shell flashes or thermal pulses generate a peak luminosity of several $10^8 L_{\odot}$. This large energy generation causes convective instability of the layer between the He- and the H-burning shells. This layer between the shells is the intershell. The convective instability driven by the He-shell flash is the pulse-driven convection zone (PDCZ). The recurrent thermal pulses, as well as the consequences for nucleosynthesis and mixing are illustrated in Fig. 6. Shown is the time evolution of the narrow region (in Lagrangian coordinates) from the top of the inert C/O core to the bottom of the envelope convection that reaches all the way to the surface. The nuclear production in thermally pulsing AGB stars is determined by the interplay of the PDCZ and the envelope convection. This interplay allows the consecutive and alternating exposure of material to He- and H-burning. It can be explained best by following the events of one full pulse cycle as shown in Fig. 6 in detail.

3.1.1. *The thermal pulse cycle*

The He-burning that provides the energy for the PDCZ is dominantly the triple- α reaction, producing ^{12}C from ^4He . In addition a larger number of additional α -capture reactions are activated. Among these is the $^{22}\text{Ne}(\alpha, n)^{25}\text{Mg}$ reaction that releases neutrons and leads to a large neutron flux at the bottom of the PDCZ. We will get to the origin of ^{22}Ne in the PDCZ in a moment. The neutron irradiation has two effects. It leads to the production of many n-rich species heavier than iron, the *s*-process elements, and at the same time it reduces the abundance of the seed species of the *s*-process, the most important of which is ^{56}Fe .

The H-shell at the bottom of the convective envelope reacts to the perturbation of the He-shell flash in a characteristic way. Due to the expansion and cooling of the layers above the He-shell, the H-shell is temporarily extinguished. After briefly receding ($0 < t < 100$ yr in Fig. 6) the convective envelope engulfs more material from deeper layers. Eventually a significant amount of material that has just been mixed and nuclear processed in the PDCZ is convectively mixed into the envelope and to the stellar surface by this third dredge-up¹. At the end of the third dredge-up the H-rich envelope and the ^{12}C -rich intershell layer are in direct contact, and any partial mixing, such as due to overshooting (Herwig et al. 1997) or internal gravity waves (Denissenkov & Tout 2003) leads to a thin layer that contains both H and ^{12}C . As this layer resumes contraction after the thermal pulse and gradually heats up, H-shell burning eventually starts again. As part of that process any partial mixing layer of H and ^{12}C will produce an excess of ^{13}C . Detailed models have revealed that the neutron release in the ^{13}C -pocket through the reaction $^{13}\text{C}(\alpha, n)^{16}\text{O}$ plays the most important role for the *s*-process in AGB stars (Gallino et al. 1998; Busso et al. 1999).

As the H-shell burns outward during the interpulse phase it leaves behind H-burning ashes, which mainly consist of ^4He . However, any CNO material in the envelope, including previously dredged-up ^{12}C will be transformed into ^{14}N . In addition the He-shell ashes contain fresh ^{56}Fe from the envelope. Just below the region with

H-shell burning ashes is a thin layer that contains the ^{13}C -pocket. The fact that the ^{13}C pocket contains a highly ^{14}N -rich region just above the ^{13}C -abundance peak is extremely important in models that include shear mixing induced by differential rotation (Herwig et al. 2003a; Siess et al. 2004). The abundance distribution in the following PDCZ is therefore a mix of the H-shell ashes, the *s*-process enriched material from the nuclear processed ^{13}C -pocket, and material that has been mixed and exposed to nucleosynthesis in the previous PDCZ. Obviously the previous PDCZ is similarly a mix of these different components. Full stellar evolution calculations including sufficiently detailed nuclear networks can generate quantitative predictions for the intershell abundance distribution after many thermal pulses.

3.1.2. *Convective extra mixing and rotation*

Convective extra mixing refers to a complex family of physical processes that lead to convection induced mixing in stable layers adjacent to a convectively unstable zone. Although convective extra mixing is sometimes referred to as simply overshooting, this term is reserved for the convective fluid motions that extend from the unstable into the stable layers, and leave the thermodynamic stratification sub-adiabatic. If convective plumes that reach into the stable layers lead to an adiabatic stratification the convective extra mixing is referred to as penetration (Zahn 1991). However, yet another physical process can convectively induce mixing beyond the convective boundary. Convective motions may perturb the convective boundary which can lead to the excitation of internal gravity waves (Press 1981). Such gravity modes can induce mixing in the radiative vicinity of convective boundaries (Garcia Lopez & Spruit 1991; Montalbán 1994; Denissenkov & Tout 2003).

Over the past decade hydrodynamic convection simulations have generated additional insight into the relative importance of these convective extra mixing processes. A very good example of overshooting has been observed in the shallow surface convection simulations by Freytag et al. (1996). Convective motions, both downdrafts and upflows cross the convective boundaries without effort. The exponential decay of the convective motions stretches over a pressure scale height.

¹The first and second dredge-up can occur earlier during the star's evolution after the H- and He-core burning ceases.

Due to the very soft convective boundary no gravity wave excitation could be observed in these simulations. Hydrodynamic simulations by Bazan & Arnett (1998) and Young et al. (2005) have shown that the oxygen-shell convection in massive stars is a different regime. Although overshooting is observed in these calculations as well, an equally important or maybe even dominating process for mixing is the excitation of gravity waves that generate turbulence in the radiative layers next to the convective boundary. The excitation of gravity waves is possible because the convective boundaries are much stiffer than in shallow surface convection. Qualitatively similar results have been found for He-shell flash convection in AGB stars by Herwig et al. (2006). Although convective extra mixing has not been analysed quantitatively, this study shows that overshooting motions are severely limited in their ability to cross the stiff convective boundary, especially the bottom boundary. However, the boundary stiffness leads to the excitation of high-amplitude gravity waves. The most recent simulations indicate that a small amount of mixing across the convective boundaries of the PDCZ exists, both at the top and at the bottom boundaries.

Convective extra mixing at the bottom of the PDCZ has been included in AGB calculations as an exponential decay of the mixing-length theory convective diffusion coefficient (Herwig et al. 1997; Althaus et al. 2005b). Such extra mixing leads to higher temperature at the bottom of the PDCZ (Herwig 2000) with implications for the *s*-process branching nucleosynthesis driven by the ^{22}Ne neutron source (Lugaro et al. 2003; Herwig et al. 2006). This limits the maximum amount of convective extra mixing at the bottom of the PDCZ, but a detailed analysis to quantify this limit is not yet available. For the H-deficient post-AGB stars another effect of this mixing is more important. The models predict that larger convective extra mixing leads to a larger intershell abundance of ^{16}O . As we will explain below, the observed oxygen abundance of H-deficient post-AGB stars are in very good agreement with AGB models that include this extra mixing at the bottom of the PDCZ. The hydrodynamic properties of convective boundaries are intimately related to the predicted abundance patterns of H-deficient post-AGB stars.

The effect of stellar rotation, on the other side, has not yet been studied in the same detail. Stellar models of AGB stars including the effect of rotation have shown that the *s*-process nucleosynthesis efficiency in the ^{13}C pocket may be reduced compared to non-rotating models (Herwig et al. 2003a; Siess et al. 2004). Indirectly, convective extra mixing at the bottom of the PDCZ could compensate for the reduced *s*-process efficiency in rotating AGB models through a larger ^{12}C intershell abundance (Herwig et al. 2006). While, as we will discuss below, such a larger ^{12}C intershell abundance is in agreement with observations of H-deficient post-AGB stars, detailed models of this scenario are not yet available. It therefore seems that stellar rotation at this point is rather indirectly relevant for the interpretation of abundance patterns of H-deficient post-AGB stars.

3.2. Post-AGB evolution

When the AGB star has lost all but approximately $10^{-2} M_{\odot}$ of its envelope mass it starts the transition from the giant configuration to the white dwarf configuration (Schönberner 1979). The remaining envelope contracts and the star evolves at constant luminosity to the hot stellar temperatures ($T_{\text{eff}} > 30\,000\text{ K}$) that are required for central stars to ionize the planetary nebulae. Mass loss plays an important role in determining the transition velocity during this phase (Blöcker 2001). Eventually hydrogen shell-burning stops and both the stellar luminosity and effective temperature start to decrease (Fig. 1). The star is about to enter the white dwarf cooling track. Up to this point the star retains the ability to ignite a He-shell flash, if the amount of He accreted from the H-shell is large enough, and the density in the He-shell is high enough. Such a post-AGB He-shell flash will initiate a born-again evolution during which the star is reborn as a giant star. The basic concept of the born-again evolution scenario was established by Iben et al. (1983) and Schönberner (1983). It is noteworthy that Iben et al. (1983) have already speculated about the existence of two distinct born-again evolution channels, to which we now refer as the late thermal pulse (LTP) and the very late thermal pulse (VLTP). We add to those a variation of single star evolution that may be able to produce (possibly only mildly) H-deficient hot post-AGB stars without a born-again

evolution, the so-called AGB final thermal pulse (AFTP).

3.2.1. VLTP

In the VLTP born-again evolution case the PDCZ (Fig. 6) is able to penetrate into the remaining H-rich envelope, triggering a H-ingestion flash (HIF) that imposes its own nuclear burning and mixing signature on the subsequent evolution (Blöcker 2001; Herwig 2001). This HIF is possible when the He-shell flash occurs very late in the post-AGB evolution, when the star is converging onto the white dwarf cooling track. At that time the H-shell is inactive, and provides no entropy jump that could prohibit convective instability below to spread outwards.

The time at which a He-shell flash can occur during the post-AGB evolution depends on the thermal pulse phase at which the star leaves the AGB. A departure too early in the cycle means that no He-shell flash will happen, a departure too late in the cycle means a He-shell flash is triggered early in the post-AGB phase when the H-shell is still on, resulting in a LTP born-again evolution, rather than a VLTP.

Most born-again models that have been presented more recently are in fact VLTP models (Iben & MacDonald 1995). The chain of events starts with the onset of the He-shell flash convection that spreads over the entire intershell as the He-burning luminosity quickly increases in thermonuclear runaway. Close to the peak luminosity the convective instability extends into the H-rich, unprocessed envelope. Protons are transported on the convective time-scale into the hot, deep layers of the PDCZ. Eventually the proton-rich material reaches temperatures that are high enough to allow the $^{12}\text{C}(p, \gamma)^{13}\text{N}$ reaction to proceed on the convective time scale. At this position within the PDCZ the peak H-burning energy will be released. If we believe the 1D-stellar evolution models the energy generation leads to the formation of a separate convection zone driven by the H-burning energy, and separated from the He-shell convection zone beneath by a small radiative layer. The upper H-burning layer probably engulfs the entire material up to the stellar surface, and burns its hydrogen content. Whatever traces of H maybe left will very likely be shed off by mass loss during the subsequent giant phase.

The VLTP model computations certainly are among the numerically more difficult stages of stellar evolution. Nevertheless, several improvements have been made in recent years. The VLTP model by Herwig et al. (1999) included a reliable, fully implicit numerical method for solving simultaneously the nuclear network and the time-dependent mixing equations. They also based their post-AGB evolution sequence on an AGB progenitor with convective extra mixing (Sect. 3.1.2). In that way the model could reproduce the observed high O abundance in [WC] and PG1159 stars. For the surface abundances, especially oxygen, Althaus et al. (2005b) come to the same conclusion.

When it became clear that Sakurai's object was in fact a VLTP case in which the born-again evolution from the pre-WD to the giant phase was witnessed in real-time (Sect. 2.4) it also became clear that this star was not following the script that had been laid out by any of the previous calculations. The born-again evolution from the He-shell flash to the giant configuration has been observed to be only about two years. However, any previous VLTP calculation predicted born-again evolution times of a factor 10 (Iben 1995) to 100 (Herwig et al. 1999) longer. An important difference between these two calculations is the numerical treatment of simultaneous burning and mixing, opacities, and metallicity, which collectively make a factor of 10 difference very plausible. For example, Lawlor & MacDonald (2003, Table 2, section D-E) show that the duration of the constant luminosity part of the born-again evolution is about three times shorter for $Z = 0.001$ compared to $Z = 0.02$. In any case, the important point is that these calculations do agree in the fact that Sakurai's object was retracing the evolution back to the AGB much faster than predicted by VLTP models. This indicated, that the born-again evolution time is sensitive to the numerics, and as well to the physics of burning and mixing, and possibly other input physics.

Subsequently a new generation of models of the VLTP has appeared. At the 2000 workshop *Sakurai's object: What have we learned in the first five years?* in Keele, UK, Lawlor & MacDonald (2002) presented VLTP tracks with two loops, similar to the track shown dashed in Fig. 1. However, the difference between these new models with double-loop (see also Herwig 2003; Hajduk et al. 2005)

and previous models was not clear initially. Then, Herwig (2001) showed a connection between the convective mixing speed of surface H into the hot He- and ^{12}C -rich layers deeper inside and the born-again evolution time from the hot pre-white dwarf stage back to the giant configuration. The Lawlor & MacDonald (2002) and the Herwig (2001) models as well as all later VLTP models use some simultaneous treatment of nuclear burning and convective time-dependent mixing in which the nuclear network equation sets in each mass shell are solved together with the diffusion equations for each species. Although the basic concept is similar in all more recent models the details of the numerical solution technique differ, with possible consequences for the calculated born-again time scale.

Herwig (2001) performed a series of tests for a $0.604 M_{\odot}$ post-AGB star with a range of mixing speeds. Peak nuclear burning of ingested H with ^{12}C should occur where the nuclear and the mixing time scales are the same. As the temperature strongly increases as protons convectively diffuse inward the nuclear time scale decreases. For reduced mixing velocity the mixing time scale is larger and the position of equality of nuclear and mixing time scales is closer to the surface than with a faster mixing velocity as predicted by the mixing-length theory. These models suggested that a solar metallicity model with a mass of $0.604 M_{\odot}$ could reproduce the born-again evolution time of Sakurai’s object if the convective mixing speed is reduced by a factor 100.

Lawlor & MacDonald (2003) discuss the effect of reducing the mixing efficiency for three values: reduction by 10^2 , 10^3 and 10^4 . This may be a different regime than the one explored by Herwig (2001), because they report a longer evolution time scale for a reduction factor 10^4 than for 10^3 . It should be noted however, that neither of these models included some possibly important physics, like the effect of μ -gradients on convective boundaries, or time-dependent convective energy transport.

The emerging picture, that was first fully described by Lawlor & MacDonald (2003), is that the VLTP evolution is a superposition of two flashes, reflected in the double loop morphology of the HRD track. The first fast born-again evolution is the result of the H-ingestion flash, whereas the

second longer lasting loop is driven by the He-shell flash that is still proceeding at the bottom of the intershell, largely unperturbed.

Even more recently, Althaus et al. (2005b) have presented new calculations of the VLTP, that connect the VLTP event with the observational properties of PG1159 stars, and DB and DQ white dwarfs. These calculations confirm the double-loop picture, and feature a born-again evolution time of 50 yr. Miller Bertolami et al. (2005) investigate the dependence of the born-again times on additional physics, like the convection theory and the μ -gradients, and on numerical aspects, like time resolution. The born-again time of their best model is 17 yr without changing the mixing velocity *ad hoc*. They do confirm the relation between mixing velocity and born-again time of Herwig (2001).

3.2.2. Discussion of the H-ingestion mixing during the VLTP

As the discussion in the previous section shows, the more recent stellar evolution studies of the VLTP show some agreement (e.g. the double-loop structure) as well as disagreement (e.g. the quantitative born-again time scale). All these calculations are based on some assumptions that are well founded in many phases of stellar evolution: spherical symmetry, convection can be described by time-averaged quantities as in mixing-length theory, hydrostatic equilibrium. However, several or maybe all of these assumptions are invalid for the VLTP. The ingestion of hydrogen into the He-shell flash convection zone is a complicated multi-dimensional problem of turbulent convective-reactive fluid flow in which composition changes and reactive energy release are coupled to the dynamics (Dimotakis 2005).

There is considerable uncertainty in the treatment of non-reactive mixing at the H-rich – C-rich interface at the top of the convection zone. Convective rising plumes will perturb this interface, possibly penetrating a small distance. The perturbation of the boundary layer induces gravity waves (Herwig et al. 2006) which cause, possibly in the interaction with a small amount of convective penetration, shear flows and thereby turbulent mixing at this interface. This boundary mixing will be very important because the much lower molecular weight of material in the

H-rich stable layer will prevent unmixed blobs to be entrained easily into the He-shell flash convection zone. Nevertheless, as any stellar convection simulation shows, including those of the He-shell flash convection of Herwig et al. (2006), the overall convective flow morphology is dominated by structures that have roughly the size of the vertical extent of the convection zone. On these large vertical scales confined downflows will eventually contain material with a significant H-abundance. Nuclear energy from the $^{12}\text{C}(p,\gamma)^{13}\text{N}$ reaction is released in localized bursts at the vertical position where the temperature is large enough to reduce the nuclear burning time scale down to the local mixing time scale. This mixing time scale corresponds to the actual velocity in the downflow, not the rms-averaged value, that corresponds in fact well with the mixing-length velocity.

In most stellar evolution situations the nuclear time scale is much longer than the convective time scale. This justifies the customary operator split between the convective mixing step and the nuclear burning calculation. It also justifies the assumption that nuclear energy release is isotropic in the horizontal direction (or on spheres). However, in the H-ingestion flash there are small and irregular parcels of energy production that coincide with the horizontal area of H-rich downflows. This breaks spherical symmetry.

The bursts of energy will locally add buoyancy and alter the convective flow patterns, deflecting focused downflows sideways or even reversing the flows. This has its correspondence to the notion derived from 1D models that the energy release from the H-ingestion flash will lead to a split of the convective region associated with an impenetrable entropy barrier. Whether or not such a separation of convection zones will actually develop in real stars, and whether the 1D mixing-length theory-based diffusion-burning models can account for this evolution phase at all is uncertain, considering the many unknown aspects of the complicated reactive, turbulent mixing that dominates the above sketched picture of the problem. This picture is based on our preliminary multi-dimensional hydrodynamic calculations of the H-ingestion problem.

In view of all these complications it seems rather surprising that the more recent 1D VLTP stellar evolution models agree to some extent with

each other, and with the observed evolution of Sakurai’s object at all. However, there is room for some doubt whether the current models describe the physics correctly on the level needed to understand the observations.

3.2.3. *LTP and AFTP*

If the He-shell flash ignites during the earlier horizontal, constant-luminosity evolution the star will follow a born-again evolution but without a hydrogen ingestion flash (HIF). This variant of the post-AGB He-shell flash is the late thermal pulse (Blöcker 2001; Blöcker & Schönberner 1997). Although the LTP does not deplete H in the surface layer by nuclear burning it will still develop a H-deficient surface composition (Herwig 2001). This is achieved entirely by mixing. As the star inflates and the surface becomes cooler, envelope convection, that is characteristic for giant stars, emerges again. At this point a dredge-up event in the same way as following the AGB thermal pulses will mix a very thin H-rich envelope layer of the order $10^{-4} M_{\odot}$ with a few $10^{-3} M_{\odot}$ of H-free intershell layer. The result is H-deficiency as a result of dilution. The LTP model of Herwig (2001) predicts a H surface mass fraction of $X_{\text{H}} = 0.02$.

The LTP has only a single loop back to the AGB which proceeds on a long time scale of the order 10^2 yr. In addition there are differences in the abundance evolution resulting from the fact that the LTP did not experience a H-ingestion flash (Sect. 3.3). These include no Li production, no enhanced ^{14}N abundance, a larger $^{12}\text{C}/^{13}\text{C}$ ratio than in the VLTP HIF models. Unfortunately there are no detailed LTP models including all relevant nucleosynthesis and a realistic treatment of the AGB progenitors available.

The born-again scenario may imply that H-deficient CSPN should have systematically older PN, which is not the case (Górny 2001). In contrast, the appeal of the AFTP scenario is that it does not require the central star to evolve through a lengthy first CSPN phase and the return to the AGB and to the CSPN again. The AFTP leads to H-deficiency at the last thermal pulse still on the AGB. By invoking some fine-tuning of the mass loss the envelope mass at the last AGB thermal pulse is so small that the star leaves the AGB immediately after the dredge-up following this last AGB thermal pulse. Because of this very small en-

velope mass the dredge-up leads as in the LTP to a significant dilution of the H surface abundance.

The AFTP scenario is in contradiction to AGB stellar evolution studies of dredge-up towards the end of the AGB evolution, which assert that dredge-up stops when the envelope mass falls below a certain value. For example, a minimum envelope mass of $0.5 M_{\odot}$ for dredge-up was reported by Straniero et al. (1997). However, dredge-up predictions in stellar evolution models are notoriously dependent on fine-tuning some mixing parameters, like the mixing-length parameter or the overshooting parameter.

The two AFTP models of Herwig (2001) were calculated with a mixing-length parameter of $\alpha_{\text{MLT}} = 3.0$ and overshooting. At the time of the last AGB thermal pulse the envelope mass was $3 \cdot 10^{-2} M_{\odot}$ and $4 \cdot 10^{-3} M_{\odot}$, and the dredged-up mass was in both cases $6 \cdot 10^{-3} M_{\odot}$. This resulted in H-abundances at the surface of the post-AGB star of $X_{\text{H}} = 0.55$ and 0.17 , respectively. This is much larger than the H-abundance observed in PG1159 stars. However, the AFTP model may explain quite naturally the “hybrid” PG1159 stars which are H-deficient but yet have H abundances much larger than the typical PG1159 and [WR]-CSPN stars (Tables 1 and 2; Napiwotzki et al. 1991).

The main problem with the AFTP scenario seems to be a missing mechanism that favors the pulse phase zero (or very small) for the departure from the AGB. Somehow, the thermal pulse must trigger enhanced mass loss that in turn enhances the probability of a departure at phase close to zero. The typical AGB mass-loss formulae do not provide such a mechanism and would lead to a very low probability of such an event.

De Marco et al. (2003b) considered the possibility that swallowing a planet or a very-low mass star companion could eject the star with high probability during the temporary, significant radius increase induced by the thermal pulse. The multi-dimensional simulations showed that envelope ejection is indeed possible. This would initialize the departure from the AGB. Clearly this interesting possibility needs more investigation, and such efforts are underway.

3.2.4. *The HRD tracks of post-AGB evolution and the importance of the AGB progenitor evolution*

The evolution tracks of an undisturbed H-normal post-AGB evolution (no-TP), an AFTP track and a VLTP track are compared in Fig. 7. All three tracks have been started from the same tip-AGB model that was evolved through all previous evolution phases from a $2 M_{\odot}$ main-sequence model. The stellar mass at the time of departure from the AGB is $0.604 M_{\odot}$. The comparison shows that surface abundance has no effect before the “knee” (the hottest point in the track) and only a small effect after the knee, where the H-normal track is slightly cooler for a given $\log g$. However, this difference should not be overemphasized, because it is largely due to a “kink” in the track that reflects the onset of the reignition of the He-shell. In the no-TP track the He-shell flash run-away does not develop. For the HRD track after the knee it seems not to matter how the star became H-deficient. The AFTP and the final CSPN evolution of the VLTP have identical tracks. This indicates that H-normal CSPN tracks can be used as a tool to determine masses from spectroscopic stellar parameters in the absence of a homogeneous grid of H-deficient tracks.

Another point that is evident from the comparison of tracks in Fig. 2 seems to be more important for accurate mass determinations. This figure shows older tracks from Schönberner (1983), Blöcker (1995) and Wood & Faulkner (1986), as well as our newer VLTP track that is also shown in Fig. 7. While the $0.605 M_{\odot}$ track from Blöcker (1995) and the $0.6 M_{\odot}$ track from Wood & Faulkner (1986) show good agreement the new $0.604 M_{\odot}$ track is at and below the knee $\Delta \log T_{\text{eff}} = 0.1 - 0.15$ hotter. This is even more surprising since the same code (although with some differences concerning nucleosynthesis and mixing) has been used for the 0.605 and the $0.604 M_{\odot}$ model.

The reason for this HRD track difference is a different dredge-up or mass-loss history or both in the AGB progenitor evolution. For the new $0.604 M_{\odot}$ track the AGB progenitor evolution includes a complete sequence of thermal pulses, a large number of which are followed by third dredge-up mixing events. These dredge-up events

lead to a smaller effective core growth, while the properties of the core itself, in particular the radius, depends to a large extent on the increasing degeneracy of the C/O core (Herwig et al. 1998; Mowlavi 1999). If an AGB evolution sequence experiences many efficient third dredge-up events the resulting post-AGB star appears in the HRD like a slightly more massive star compared to the same core mass post-AGB stellar model that has an AGB thermal pulse history of inefficient or no dredge-up.

Mass loss can have a similar effect because it determines the age of the core for a given initial mass at the tip of the AGB (Blöcker & Schönberner 1990). This was shown in detail by Blöcker (1995, his Fig. 10) who calculated two post-AGB tracks with identical mass ($0.84 M_{\odot}$), one with a $5 M_{\odot}$ main-sequence progenitor, and one with initially $3 M_{\odot}$. In order for the $3 M_{\odot}$ model to reach such a high core mass, a smaller mass-loss rate than for the $5 M_{\odot}$ track was adopted. In this way the core had a long time to grow through shell burning before the envelope loss forced the AGB departure. The result is a more degenerate, more compact, and consequently hotter post-AGB stellar model with the $3 M_{\odot}$ progenitor compared to the post-AGB model with the $5 M_{\odot}$ progenitor.

In summary, if CSPN tracks are computed for the purpose of determining masses (or fading times) the third dredge-up and the mass loss during the progenitor evolution must be accurately taken into account.

3.3. Surface abundance predictions for H-deficient post-AGB stars

If we interpret H-deficient post-AGB stars, like PG 1159 stars or [WC]-CSPN as the bare cores of former AGB stars exposed by the born-again evolution or an AFTP evolution, then the surface abundance of these stars is a superposition of the intershell abundance of the progenitor AGB star at the last thermal pulse on the AGB and any modification that in particular the violent burning and mixing associated with the H-ingestion flash of the VLTP may have caused. In the following we discuss the surface abundance predictions for the elements that have been observed so far, taking into account both of these contributions.

3.3.1. Carbon and Oxygen

During the He-shell flash the triple- α reaction that transforms three ${}^4\text{He}$ into one ${}^{12}\text{C}$ is the dominant source of energy. The layers immediately below the PDCZ contain an amount of ${}^{16}\text{O}$ from the ${}^{12}\text{C}(\alpha, \gamma){}^{16}\text{O}$ reaction, increasing with depth. Starting with the earliest models of thermal pulse AGB stars (Schönberner 1979) it has been consistently found that without convective extra mixing the ${}^{16}\text{O}$ abundance is 0.01–0.02, and the ${}^{12}\text{C}$ abundance is 0.2–0.25 in the intershell with the remaining ~ 0.75 ${}^4\text{He}$.

More recently models with convective extra mixing in the form of a parameterized exponential overshoot at the bottom of the PDCZ have been constructed (Herwig et al. 1997; Herwig 2000; Althaus et al. 2005b). These models agree quantitatively that such extra mixing leads to a systematically larger ${}^{16}\text{O}$ and ${}^{12}\text{C}$ abundance in the PDCZ. Herwig (2000) showed that the efficiency of convective extra mixing is proportional to the intershell ${}^{16}\text{O}$ abundance. In addition, there is an evolution of the ${}^{16}\text{O}$ abundance with pulse number, initially rising, then reaching a maximum value after a few thermal pulses and decreasing towards a plateau at the last thermal pulses. For the evolution sequence with initially $3 M_{\odot}$ Herwig (2000) finds at the last computed thermal pulse an intershell abundance of $X({}^{16}\text{O}) = 0.18$ and $X({}^{12}\text{C}) = 0.41$. For a sequence with initially $2.7 M_{\odot}$ Althaus et al. (2005b) find $X({}^{16}\text{O}) = 0.23$ and $X({}^{12}\text{C}) = 0.50$. Presumably this difference is due to the smaller number of thermal pulses in Althaus et al. (2005b) compared to Herwig (2000). As mentioned above the ${}^{16}\text{O}$ intershell abundance goes through a maximum (corresponding to a minimum for ${}^4\text{He}$) before approaching a plateau. The Althaus et al. (2005b) intershell abundance may correspond to a thermal pulse closer to that maximum.

3.3.2. Nitrogen

Nitrogen is produced in AGB stars by H-shell burning on envelope material enriched by carbon dredge-up after previous thermal pulses. In low-mass AGB stars the H-burning shell burns most CNO material in the envelope material it consumes, into ${}^{14}\text{N}$. Therefore, the H-shell burning ashes (see Fig. 6) contain with each dredge-up

pulse more ^{14}N , that is mixed in the next He-shell flash convection zone. In the He-burning shell during the flash this ^{14}N is destroyed and forms ^{18}O and ^{22}Ne (see below). The models predict that the intershell of AGB stars at the end of their evolution is practically free of ^{14}N .

In massive AGB stars ^{14}N is produced in the envelopes by hot-bottom burning (Sackmann & Boothroyd 1992). The dredged-up carbon in the envelope is transformed by two p-captures into ^{14}N because part of the H-burning shell is included in the convective envelope. Therefore, we expect in the more massive post-AGB stars of roughly solar metallicity a nitrogen mass fraction of 1% to maybe a few % in the H-rich envelope at the time of departure from the AGB.

The nitrogen evolution is different for the LTP and VLTP. The LTP will only dilute some inter-shell material with the remaining small amount of envelope material. Even if the progenitor has evolved through the hot-bottom burning phase, the nitrogen abundance will be at most roughly 0.1%. If the star evolves through a VLTP, nitrogen is produced by the H-ingestion and may be as high as a few %. The absence or presence of N should be a reliable indicator of a LTP or VLTP event.

3.3.3. Neon

During each interpulse phase the H-shell builds a layer of ashes, that is engulfed into the following PDCZ. These H-shell ashes contain mainly ^4He , with an important modification of the CNO abundances. All CNO, be it from the stellar initial abundance or dredged-up after a previous thermal pulse, will be mostly transformed into ^{14}N . This ^{14}N is exposed to the high He-burning temperature ($T \approx 3 \cdot 10^8$ K) where two α captures lead to the formation of ^{18}O first and then ^{22}Ne . Depending on mass some ^{22}Ne is destroyed by the neutron producing reaction $^{22}\text{Ne}(\alpha, n)^{25}\text{Mg}$. For low-mass AGB stars with initial masses around $1.5 M_{\odot}$ the ^{22}Ne depletion is only small ($\approx 3\%$) because the peak temperature at the base of the PDCZ is not reaching high enough values $> 3 \cdot 10^9$ K. Stellar evolution models agree that the mass fraction of ^{22}Ne is about 2%. A certain spread in the observed values is expected. The production of ^{22}Ne is larger in cases with more dredge-up of ^{12}C . The destruction of ^{22}Ne through α -capture

increases with initial mass. As a trend the inter-shell ^{22}Ne should decrease with increasing initial stellar mass.

3.3.4. Iron and Nickel

Fresh ^{56}Fe is added to the intershell with the H-shell ashes, which are processed envelope material and therefore contain the Fe-abundance of the envelope. During the PDCZ ^{56}Fe will be reduced by neutron capture and transformed into Ni if the ^{22}Ne neutron source is active, i.e. ^{56}Fe reduction will be more efficient in higher core-mass AGB stars. However, as it is the case for many other species, the evolution of ^{56}Fe in the intershell with increasing pulse number depends sensitively on the dredge-up history, which in turn seems in model calculations to be related to assumptions about convective extra mixing (Mowlavi 1999).

Preliminary models by Herwig et al. (2003b) show that the ^{56}Fe depletion in the PDCZ at the last thermal pulse of a $3 M_{\odot}$ star varies significantly depending on stellar evolution model assumptions. For a thermal pulse AGB sequence with convective extra mixing, showing very efficient third dredge-up and high peak temperatures at the base of the PDCZ, the ^{56}Fe depletion is approximately 0.7dex, whereas a model without convective extra mixing predicts a ^{56}Fe depletion of only 0.2dex. In both cases all heavier isotopes of Fe and Ni are significantly overabundant. An additional depletion of Fe and production of Ni may be obtained during the late thermal pulse (Sect. 3.2.1). In any case, the unmistakable signature of Fe depletion due to n-capture nucleosynthesis is the simultaneous increase of Ni, and correspondingly a decrease of the Fe/Ni ratio. While the solar ratio is about 20, material that has experienced a significant neutron exposure would show a ratio closer to the s-process quasi steady-state of ≈ 3 .

3.3.5. Fluorine

Jorissen et al. (1992) have observed high enhancements of fluorine in AGB stars. They found a correlation of F enhancement and C/O ratio, which is a strong indication that F is produced in the intershell and mixed to the surface during the third dredge-up. Observations show that thermal pulses cause a 10-fold increase in ^{19}F .

The nucleosynthesis path to ^{19}F first involves the production of ^{15}N which requires a neutron source: $^{14}\text{N}(n, p)^{14}\text{C}(\alpha, \gamma)^{18}\text{O}(p, \alpha)^{15}\text{N}$. This chain of reaction occurs during the interpulse phase. The neutrons are provided both by ^{13}C in the H-shell ashes, and in the ^{13}C pocket. For a certain range of mixing efficiencies, rotation induced mixing may enhance the production of ^{15}N (Herwig et al. 2003a). ^{15}N produced in either way is then engulfed by the PDCZ. F is produced by $^{15}\text{N}(\alpha, \gamma)^{19}\text{F}$. The limiting factor in this scenario is the efficient $^{19}\text{F}(\alpha, p)^{22}\text{Ne}$ reaction. ^{19}F -production exceeds destruction only in a narrow temperature range at the base of the PDCZ, between 2.2 and $2.6 \cdot 10^8$ K (Mowlavi et al. 1996).

Lugaro et al. (2004) show that the ^{19}F abundance in the He-intershell after the last thermal pulse has a maximum between 2 and $3.5 M_{\odot}$ depending on metallicity. For $Z = 0.02$ and $Z = 0.008$ the intershell abundance reaches a maximum between 150 and 290 times solar ($X(^{19}\text{F})_{\odot} = 4.1 \cdot 10^{-7}$) at 3.5 and $3.0 M_{\odot}$, respectively. However, for cores with larger or smaller initial mass the ^{19}F intershell abundance may be as small as the solar value.

Within an evolution sequence of thermal pulses for a given initial mass, and even within an individual thermal pulse the ^{19}F intershell shows a considerable spread. The variation from pulse to pulse means that a quantitative comparison with observed ^{19}F values in H-deficient post-AGB stars depends on details of the entire AGB evolution, including for example an accurate description of mass loss and dredge-up to correctly model the total number of thermal pulses. The spread within one He-shell flash convection event means that there may be observable differences in the ^{19}F abundance between VLTP with H-ingestion and LTP born-again evolutions.

Finally it should be mentioned that Lugaro et al. (2004) find that nuclear reaction rate uncertainties, in particular of the $^{14}\text{C}(\alpha, \gamma)^{18}\text{O}$ and the $^{19}\text{F}(\alpha, p)^{22}\text{Ne}$ reactions, significantly limit the accuracy of stellar model predictions of ^{19}F .

3.3.6. Si, P and S

These three elements have a too high Coulomb barrier to be altered by charged particle reactions in AGB stars. This leaves only neutron captures

to be considered for elemental abundance shifts of Si, S and P. It is well known from the study of pre-solar grains, that the neutron fluxes in AGB stars modify the ratios of the three stable Si isotopes (Lugaro et al. 1999). However, the elemental abundance of Si is dominated by the lightest isotope, ^{28}Si , which in the solar abundance distribution accounts for approximately 90% of the elemental Si abundance. Neutron exposure in AGB stars will shift a small fraction of ^{28}Si to ^{29}Si and ^{30}Si , but the elemental abundance changes only very little in the He intershell of AGB stars. Therefore, a solar Si abundance is expected in hot H-deficient post-AGB stars.

For P the model calculation with initially $3 M_{\odot}$ predicts an enhancement in the intershell at the end of the AGB that is sensitive to the assumptions about convective extra mixing. The expected range is from four times solar without extra mixing to ~ 25 times solar with extra mixing. As discussed in Sect. 3.1.2 the respective mixing algorithm contains a free efficiency parameter. We consider the efficiency chosen in this model an upper boundary. As it is the case for ^{19}F , the He-shell flash nucleosynthesis can be sensitive to the initial mass. A systematic evaluation of the P intershell abundance as a function of mass and metallicity is not yet available.

The same models predict a small deficiency in S in the intershell at the end of the AGB, ranging from 0.6 times solar with convective extra mixing to 0.9 times solar for the standard model. A more systematic evaluation of the intershell abundance evolution of S and P should include the neutron capture cross section uncertainties. However, in general the uncertainties for these stable isotopes are typically less than 10% (Bao et al. 2000).

3.3.7. Lithium

Although Li can not be observed in hot post-AGB stars, the observed Li overabundance in Sakurai's object is an important hint. The production of this fragile element in the form of its heavy isotope ^7Li is usually associated with hot-bottom burning in massive AGB stars (Scalo et al. 1975; Sackmann & Boothroyd 1992). Enhanced extra mixing in red giant branch stars induced by tidal synchronization or swallowing of a giant planet has been proposed as another source of ^7Li (Denisenkov & Herwig 2004). Both of these produc-

tion sites are based on the ${}^7\text{Be}$ transport processes. ${}^3\text{He}$ and ${}^4\text{He}$ form ${}^7\text{Be}$ which becomes ${}^7\text{Li}$ through a largely temperature insensitive e^- -capture on a time-scale of approximately one year. If the production region of ${}^7\text{Be}$ is convectively connected to cooler layers, like in envelope convection that reaches into the H-burning shell in hot-bottom burning, then ${}^7\text{Be}$ is transported out of the hot layers, and the resulting ${}^7\text{Li}$ can survive, because it is not immediately destroyed by p-captures.

Herwig & Langer (2001) have shown that if ${}^3\text{He}$ in the envelope has not been destroyed by one of the two processes mentioned above (which is likely for most low-mass AGB stars with initial masses below $\sim 3.5 M_{\odot}$), then copious amounts of ${}^7\text{Li}$ can be produced in the hydrogen ingestion flash. They refer to this process as hot H-deficient ${}^3\text{He}$ burning. The reason is somewhat different from the ${}^7\text{Be}$ transport mechanism, in which ${}^7\text{Be}$ is transported out of the hot p-rich, and therefore ${}^7\text{Li}$ hostile environment quickly enough. In the HIF the amount of ingested H is strictly limited, and in addition to H, ${}^3\text{He}$ is ingested into the He-shell flash convection zone. This ${}^3\text{He}$ quickly reacts with ${}^4\text{He}$ and forms ${}^7\text{Be}$, which then has to wait for an e^- capture to become ${}^7\text{Li}$. This waiting period is long enough for all the protons to be rapidly consumed by ${}^{12}\text{C}$. By the time ${}^7\text{Li}$ appears no protons are available anymore for Li destruction, leading to a net production of ${}^7\text{Li}$. Current models only account qualitatively for the processes involved. In a one-zone model Herwig & Langer (2001) find a maximum mass fraction of $X({}^7\text{Li}) = 3 \cdot 10^{-6}$, which corresponds to $\sim 2.5\text{dex}$ more than the solar system meteoritic value. We expect that the surface overabundance of Li in a realistic multi-zone model would be much smaller.

${}^7\text{Li}$ production in a HIF has been recently confirmed by Iwamoto et al. (2004) in the context of He-shell flashes in extremely metal-poor AGB stars. In this context it is interesting to note that Cameron & Fowler (1971) in fact originally proposed the ${}^7\text{Be}$ transport mechanism motivated by the first HIF models by Schwarzschild & Härm (1967) that were, however, not reproduced by subsequent models that included radiation pressure.

4. Comparison of observation and theory

In the previous Sections 2 and 3 we have presented in detail the element abundances observed in PG1159 and [WC] stars as well as the the surface abundances predicted from stellar evolution models. How do they compare?

Hydrogen: The observed H deficiency is in accordance with evolution models of the born-again scenario. In the VLTP models H is ingested and burned and disappears completely. An LTP event causes mixing of the H-rich envelope with the intershell so that H is diluted down to a mass fraction of the order 0.02. This is close to the observational limit. The relatively high H abundances in the hybrid-PG1159 stars and some [WC] stars (of the order 0.15) are explained by AFTP models.

Helium, carbon and oxygen: These are the main constituents of the intershell region of AGB stars and the model abundances generally agree with the observed abundances in PG1159 and [WC] stars. The spread of observed relative He/C/O ratios can in part be explained by differences in stellar mass and the different number of thermal pulses experienced by objects even with equal total mass (the latter being a consequence of potentially different AGB mass-loss, for example as a result of rotation). However, we think that some few extreme cases of He/C/O ratios remain unexplained, in particular objects with relatively low O abundance (of order 0.01) and simultaneously high C abundance (of order 0.5). One speculative scenario has been sketched by De Marco et al. (2003a). If the AGB star has a low-mass stellar or planetary companion at a distance of 1–2 AU it would be engulfed during the radius peak induced by the first thermal pulse. The transfer of orbital energy into the AGB envelope may eject the envelope and lead to a departure from the AGB. According to Herwig (2000) the intershell O abundance is very low after the first thermal pulse even if overshooting has been applied. If such an evolution later involves a VLTP or LTP, a PG1159 star with a very low O abundance would result. A similar evolution could result from a low-mass star that naturally leaves the AGB just before the first thermal pulse (Miller Bertolami & Althaus 2006).

Isotopic ratios can not be measured in hot post-AGB stars. However, both the ${}^{12}\text{C}/{}^{13}\text{C}$ and the

C/N ratios of our VLTP model are in good agreement with the observations of Sakurai's object.

Nitrogen: The observations show a wide range of N abundance, from very low upper limits ($< 3 \cdot 10^{-5}$ in HS1517+7403) to mass fractions of 1–2%, in agreement with predictions for LTP and VLTP evolution, respectively. Intermediate abundance levels could in some cases be associated with higher stellar mass.

Neon: The observed high Ne abundances (of the order 0.02) agree well with the model predictions.

Fluorine: The rich diversity of F abundances observed in PG1159 stars (from solar up to 250 times solar) is explained by models with different stellar mass leading to different F production efficiencies.

Silicon: The Si abundance in the evolution models is almost unchanged so that a solar abundance is expected. Only few abundance analyses are available. PG1159 stars display the expected Si abundance while surprisingly strong overabundances (up to 40 times solar) were found in some [WCL] stars.

Phosphorus: Theoretical predictions and observational data are scarce. Current models are consistent with P overabundances of up to 4–25 times solar. Preliminary results from two PG1159 stars indicate roughly solar abundances.

Sulfur: Preliminary abundance determinations in PG1159 stars suggest a wide spread, ranging between 0.01–1 times solar. These results need to be confirmed by further analyses. Like in the case of P, systematic investigations with evolution models are lacking, but current models predict only slight (0.6 solar) S depletion.

Lithium: The Li abundance cannot be determined in hot objects so that no conclusions can be drawn from PG1159 and [WC] stars. Sakurai's object, however, shows a large Li abundance. As discussed in previous sections this Li can not have survived from an earlier phase, and is a strong additional hint that Sakurai's object did in fact evolve through a VLTP.

Iron and Nickel: The observed Fe deficiency in PG1159 and [WC] stars is explained by neutron captures on ^{56}Fe . The consequent increase of the Ni abundance cannot be confirmed or contradicted with current observational material. However,

Sakurai's object indeed exhibits a strongly sub-solar Fe/Ni ratio, that is quantitatively in agreement with model estimates.

To conclude, element abundances predicted by born-again evolutionary models (LTP and VLTP case) as well as the AGB Final Thermal Pulse models (AFTP case) can explain most observational results from PG1159 and [WC] star analyses. The model surface abundances largely reflect the intershell abundance of the AGB progenitor. From the good qualitative and quantitative agreement between observed and predicted abundances we conclude that [WC] and PG1159 stars generally display on their surface the intershell material of the AGB progenitor. For this reason, detailed quantitative spectroscopic investigations of these hot post-AGB stars can be used as a tool to study the nuclear production site of the He-intershell in AGB stars. Such a tool is in particular useful because the AGB interior is otherwise obviously inaccessible to direct observation. It is hoped that new observations and analyses of these H-deficient post-AGB stars will contribute to an even more complete picture of the nuclear astrophysics processes in AGB stars.

F.H. would like to thank Lars Koesterke for his early support in numerical methods for burning and mixing in 1D born-again stellar evolution models. He would also like to thank Bernd Freytag for their delightful collaboration on stellar interior convection hydrodynamic simulations, and Orsola De Marco for many enlightening discussions about CSPN and other things. K.W. thanks Stefan Dreizler, Uli Heber, and Thomas Rauch for their enduring close collaboration. We would like to thank Maria Lugaro for her help with preliminary estimates on P and S abundance predictions. Comments on an earlier version of this paper by Orsola De Marco, Wolf-Rainer Hamann, Thomas Rauch, and Detlef Schönberner are gratefully acknowledged. This work was funded in part under the auspices of the U.S. Dept. of Energy under the ASC program and the LDRD program (20060357ER) at Los Alamos National Laboratory. It was also funded in part by the German Science Foundation (DFG) and the German Aerospace Center (DLR). Fig. 1 and Fig. 6 with minor modifications are reprinted, with permission, from the Annual Review of Astronomy and

Astrophysics, Volume 43 (c) 2005 by Annual Reviews www.annualreviews.org.

REFERENCES

- Acker, A. & Neiner, C. 2003, *A&A*, 403, 659
- Althaus, L. G., Miller Bertolami, M. M., Córscico, A. H., García-Berro, E., & Gil-Pons, P. 2005a, *A&A*, 440, L1
- Althaus, L. G., Serenelli, A. M., Panei, J. A., Córscico, A. H., García-Berro, E., & Scóccola, C. G. 2005b, *A&A*, 435, 631
- Asplund, M., Gustafsson, B., Lambert, D. L., & Rao, N. K. 2000, *A&A*, 353, 287
- Asplund, M., Lambert, D. L., Kipper, T., Pollacco, D., & Shetrone, M. D. 1999, *A&A*, 343, 507
- Bao, Z. Y., Beer, H., Käppeler, F., Voss, F., Wisshak, K., & Rauscher, T. 2000, *ADNDT*, 76, 70
- Barlow, M. J. & Hummer, D. G. 1982, in *Wolf-Rayet Stars: Observations, Physics, Evolution*, ed. C. de Loore & A. Willis, IAU Symp. 99 (Dordrecht: Reidel), 387
- Bauer, F. & Husfeld, D. 1995, *A&A*, 300, 481
- Bazan, G. & Arnett, D. 1998, *ApJ*, 496, 316
- Blöcker, T. 1995, *A&A*, 299, 755
- Blöcker, T. 2001, *Ap&SS*, 275, 1
- Blöcker, T. & Schönberner, D. 1990, *A&A*, 240, L11
- . 1997, *A&A*, 324, 991
- Bond, H. E., Kawaler, S. D., Ciardullo, R., Stover, R., Kuroda, T., Ishida, T., Ono, T., Tamura, S., Malasan, H., Yamasaki, A., Hashimoto, O., Kambe, E., Takeuti, M., Kato, T., Kato, M., Chen, J.-S., Leibowitz, E. M., Roth, M. M., Soffner, T., & Mitsch, W. 1996, *AJ*, 112, 2699
- Busso, M., Gallino, R., & Wasserburg, G. J. 1999, *ARA&A*, 37, 239
- Cameron, A. G. W. & Fowler, W. A. 1971, *ApJ*, 164, 111
- Clayton, G. C. & De Marco, O. 1997, *AJ*, 114, 2679
- Córscico, A. H. & Althaus, L. G. 2005, *A&A*, 439, L31
- Cox, A. N. 2003, *ApJ*, 585, 975
- Crowther, P. A., de Marco, O., & Barlow, M. J. 1998, *MNRAS*, 296, 367
- De Marco, O. & Barlow, M. J. 2001, *Ap&SS*, 275, 53
- De Marco, O., Sandquist, E. L., Mac Low, M., Herwig, F., & Taam, R. E. 2003a, in *The eighth Texas-Mexico Conference on Astrophysics: Energetics of Cosmic Plasmas*, 24
- De Marco, O., Sandquist, E. L., Mac Low, M.-M., Herwig, F., & Taam, R. E. 2003b, in *Revista Mexicana de Astronomia y Astrofisica Conference Series*, Vol. 15, 34
- Denissenkov, P. A. & Herwig, F. 2004, *ApJ*, 612, 1081
- Denissenkov, P. A. & Tout, C. A. 2003, *MNRAS*, 340, 722
- Dimotakis, P. E. 2005, *Annu. Rev. Fluid Mech.*, 37, 329
- Dreizler, S. 1998, *Baltic Astronomy*, 7, 71
- Dreizler, S. & Heber, U. 1998, *A&A*, 334, 618
- Dreizler, S., Werner, K., & Heber, U. 1995, in *White Dwarfs*, ed. D. Koester & K. Werner, LNP No. 443 (Heidelberg: Springer), 160
- Duerbeck, H. W. & Benetti, S. 1996, *ApJ Lett.*, 468, L111
- Duerbeck, H. W., Benetti, S., Gautchy, A., van Genderen, A. M., Kemper, C., Lillier, W., & Thomas, T. 1997, *AJ*, 114, 1657
- Duerbeck, H. W., Liller, W., Sterken, C., Benetti, S., van Genderen, A. M., Arts, J., Kurk, J. D., Janson, M., Voskes, T., Brogt, E., Arentoft, T., van der Meer, A., & Dijkstra, R. 2000, *AJ*, 119, 2360
- Fedrow, J., Clayton, G., Crowther, P., & Kerber, F. 2005, AAS meeting 207, #182.20

- Fogel, J., Marco, O. D., & Jacoby, G. 2003, in *Planetary Nebulae: Their Evolution and Role in the Universe*, ed. S. Kwok, M. Dopita, & R. Sutherland, ASP, IAU Symp. 209, 235
- Freytag, B., Ludwig, H.-G., & Steffen, M. 1996, *A&A*, 313, 497
- Fu, J.-N. & Vauclair, G. 2006, *A&A*, submitted.
- Fujimoto, M. Y. 1977, *PASJ*, 29, 331
- Gallino, R., Arlandini, C., Busso, M., Lugaro, M., Travaglio, C., Straniero, O., Chieffi, A., & Limongi, M. 1998, *ApJ*, 497, 388
- Garcia Lopez, R. J. & Spruit, H. C. 1991, *ApJ*, 377, 268
- Gautschy, A. 1997, *A&A*, 320, 811
- Gautschy, A., Althaus, L. G., & Saio, H. 2005, *A&A*, 438, 1013
- Gehrz, R. D., Woodward, C. E., Temim, T., Lyke, J. E., & Mason, C. G. 2005, *ApJ*, 623, 1105
- Gonzalez, G., Lambert, D. L., Wallerstein, G., Rao, N. K., Smith, V. V., & McCarthy, J. K. 1998, *ApJS*, 114, 133
- Górny, S. K. 2001, *Ap&SS*, 275, 67
- Gräfener, G., Hamann, W.-R., & Peña, M. 2003, in *Planetary Nebulae: Their Evolution and Role in the Universe*, ed. S. Kwok, M. Dopita, & R. Sutherland, ASP, IAU Symp. 209, 577
- Grevesse, N. & Sauval, A. J. 2001, in *Encyclopedia of Astronomy and Astrophysics* (IOP Publishing Ltd. and Nature Publishing Group), 2453
- Hajduk, M., Zijlstra, A. A., Herwig, F., van Hoof, P. A. M., Kerber, F., Kimeswenger, S., Polacco, D. L., Evans, A., Lopéz, J. A., Bryce, M., Eyres, S. P. S., & Matsuura, M. 2005, *Science*, 308, 231
- Hamann, W.-R. 1997, in *Planetary Nebulae*, IAU Symp. 180, ed. H. J. Habing & H. J. G. L. M. Lamers (Kluwer), 91
- Hamann, W.-R. 2003, in *Planetary Nebulae: Their Evolution and Role in the Universe*, ed. S. Kwok, M. Dopita, & R. Sutherland, ASP, IAU Symp. 209, 203
- Hamann, W.-R., Peña, M., Gräfener, G., & Ruiz, M. T. 2003, *A&A*, 409, 969
- Hamann, W.-R., Todt, H., & Gräfener, G. 2005, in *AIP Conference Proceedings*, Vol. 804, *Planetary Nebulae as Astronomical Tools*, ed. R. Szczerba, G. Stasińska, & S. K. Górny, 153
- Heap, S. R. 1975, *ApJ*, 196, 195
- Herald, J. E., Bianchi, L., & Hillier, D. J. 2005, *ApJ*, 627, 424
- Herwig, F. 2000, *A&A*, 360, 952
- . 2001, *ApJ Lett.*, 554, L71
- Herwig, F. 2001, *Ap&SS*, 275, 15
- Herwig, F. 2003, in *Planetary Nebulae: Their Evolution and Role in the Universe*, ed. S. Kwok, M. Dopita, & R. Sutherland, ASP, IAU Symp. 209, 111
- Herwig, F. 2005, *ARA&A*, 43, 435
- Herwig, F., Blöcker, T., Langer, N., & Driebe, T. 1999, *A&A*, 349, L5
- Herwig, F., Blöcker, T., Schönberner, D., & El Eid, M. F. 1997, *A&A*, 324, L81
- Herwig, F., Freytag, B., Hueckstaedt, R. M., & Timmes, F. X. 2006, *ApJ*, in press
- Herwig, F. & Langer, N. 2001, *Nuclear Physics A*, 688, 221
- Herwig, F., Langer, N., & Lugaro, M. 2003a, *ApJ*, 593, 1056
- Herwig, F., Lugaro, M., & Werner, K. 2003b, in *Planetary Nebulae: Their Evolution and Role in the Universe*, ed. S. Kwok, M. Dopita, & R. Sutherland, ASP, IAU Symp. 209, 85
- Herwig, F., Schönberner, D., & Blöcker, T. 1998, *A&A*, 340, L43
- Hügelmeier, S. D., Dreizler, S., Homeier, D., Krzesiński, J., Werner, K., & et al. 2006, *A&A*, submitted.
- Hügelmeier, S. D., Dreizler, S., Werner, K., Krzesiński, J., Nitta, A., & Kleinman, S. J. 2005, *A&A*, 442, 309

- Iben, Jr., I. 1995, *Physics Reports*, 250, 1
- Iben, Jr., I., Kaler, J. B., Truran, J. W., & Renzini, A. 1983, *ApJ*, 264, 605
- Iben, Jr., I. & MacDonald, J. 1995, in *LNP Vol. 443: White Dwarfs*, ed. D. Koester & K. Werner (Heidelberg: Springer), 48
- Iben, Jr., I. & Renzini, A. 1983, *ARA&A*, 21, 271
- Iwamoto, N., Kajino, T., Mathews, G. J., Fujimoto, M. Y., & Aoki, W. 2004, *ApJ*, 602, 378
- Jahn, D. 2005, Diploma Thesis, University of Tübingen, Germany
- Jorissen, A., Smith, V. V., & Lambert, D. L. 1992, *A&A*, 261, 164
- Kawaler, S. D. & Bradley, P. A. 1994, *ApJ*, 427, 415
- Kawaler, S. D., O'Brien, M. S., Clemens, J. C., & et al. 1995, *ApJ*, 350, 363
- Kawaler, S. D., Potter, E. M., Vučković, M., & et al. 2004, *A&A*, 428, 969
- Koesterke, L. 2001, *Ap&SS*, 275, 41
- Koesterke, L., Dreizler, S., & Rauch, T. 1998, *A&A*, 330, 1041
- Koesterke, L. & Hamann, W.-R. 1997, in *Planetary Nebulae*, ed. H. J. Habing & H. J. G. L. M. Lamers, *IAU Symp. 180* (Dordrecht: Kluwer), 114
- Koesterke, L. & Hamann, W. R. 1997, *A&A*, 320, 91
- Koesterke, L. & Werner, K. 1998, *ApJ Lett.*, 500, 55
- Lawlor, T. M. & MacDonald, J. 2002, *Ap&SS*, 279, 123
- . 2003, *ApJ*, 583, 913
- Lechner, M. F. M. & Kimeswenger, S. 2004, *A&A*, 426, 145
- Leuenhagen, U. & Hamann, W.-R. 1998, *A&A*, 330, 265
- Lugaro, M., Herwig, F., Lattanzio, J. C., Gallino, R., & Straniero, O. 2003, *ApJ*, 586, 1305
- Lugaro, M., Ugalde, C., Karakas, A. I., Görres, J., Wiescher, M., Lattanzio, J. C., & Cannon, R. C. 2004, *ApJ*, 615, 934
- Lugaro, M., Zinner, E., Gallino, R., & Amari, S. 1999, *ApJ*, 527, 369
- Méndez, R. H. 1991, in *Evolution of Stars: The Photospheric Abundance Connection*, *IAU Symp. 145*, ed. G. Michaud & A. Tutukov, 375
- Metcalf, T. S., Nather, R. E., Watson, T. K., Kim, S.-L., Park, B.-G., & Handler, G. 2005, *A&A*, 435, 649
- Miksa, S., Deetjen, J. L., Dreizler, S., Kruk, J. W., Rauch, T., & Werner, K. 2002, *A&A*, 389, 953
- Miller Bertolami, M. M. & Althaus, L. G. 2006, *A&A*, submitted
- Miller Bertolami, M. M., Serenelli, L. G. A. A. M., & Panei, J. A. 2005, *A&A*, in press, astro-ph/0511406
- Montalban, J. 1994, *A&A*, 281, 421
- Morgan, D. H., Parker, Q. A., & Cohen, M. 2003, *MNRAS*, 346, 719
- Mowlavi, N. 1999, *A&A*, 344, 617
- Mowlavi, N., Jorissen, A., & Arnould, M. 1996, *A&A*, 311, 803
- Nagel, T., Schuh, S., Kusterer, D.-J., Stahn, T., Hügelmeyer, S. D., Dreizler, S., Gänsicke, B., & Schreiber, M. 2006, *A&A*, submitted.
- Napiwotzki, R. 1999, *A&A*, 350, 101
- Napiwotzki, R. & Schönberner, D. 1995, *A&A*, 301, 545
- Napiwotzki, R., Schönberner, D., & Weidemann, V. 1991, *A&A*, 243, L5
- Pandey, G., Lambert, D. L., Jeffery, C. S., & Kameswara Rao, N. 2005, *ApJ*, in press, astro-ph/0510161
- Press, W. H. 1981, *ApJ*, 245, 286
- Quirion, P. O., Fontaine, G., & Brassard, P. 2004, *ApJ*, 610, 436
- . 2005a, *A&A*, 441, 231

- . 2005b, *Mem. Soc. Astron. Ital.*, 75, 282
- Rauch, T., Dreizler, S., & Wolff, B. 1998, *A&A*, 338, 651
- Rauch, T., Heber, U., Hunger, K., Werner, K., & Neckel, T. 1991, *A&A*, 241, 457
- Rauch, T. & Werner, K. 1995, in *LNP Vol. 443: White Dwarfs*, ed. D. Koester & K. Werner (Heidelberg: Springer), 186
- Reiff, E., Jahn, D., Rauch, T., Werner, K., Kruk, J. W., & Herwig, F. 2006, in *ASP Conference Series*, ed. C. A. C. Sterken, in press
- Reiff, E., Rauch, T., Werner, K., & Kruk, J. 2005, in *ASP Conf. Ser. 334: White Dwarfs*, ed. D. Koester & S. Moehler, 173
- Sackmann, I.-J. & Boothroyd, A. I. 1992, *ApJ*, 392, L71
- Saio, H. 1996, in *ASP Conference Series, Vol. 96, Hydrogen-Deficient Stars*, ed. U. Heber & C. Jeffery, 361
- Saio, H. & Jeffery, C. S. 2002, *MNRAS*, 333, 121
- Scalo, J. M., Despain, K. H., & Ulrich, R. K. 1975, *ApJ*, 196, 805
- Schönberner, D. 1979, *A&A*, 79, 108
- . 1983, *ApJ*, 272, 708
- Schönberner, D. & Jeffery, C. S. 2002, in *ASP Conf. Ser. 279: Exotic Stars as Challenges to Evolution*, *IAU Coll. 279*, ed. C. A. Tout & W. Van Hamme, 173
- Schwarzschild, M. & Härm, R. 1967, *ApJ*, 150, 961
- Seitter, W. C. 1987a, *Mitteilungen der Astronomischen Gesellschaft Hamburg*, 68, 244
- . 1987b, *The Messenger*, 50, 14
- Siess, L., Goriely, S., & Langer, N. 2004, *A&A*, 415, 1089
- Smith, L. F. & Aller, L. H. 1969, *ApJ*, 157, 1245
- Starrfield, S., Cox, A. N., Hodson, S. W., & Pesnelli, W. D. 1983, *ApJ Lett.*, 268, 27
- Straniero, O., Chieffi, A., Limongi, M., Busso, M., Gallino, R., & Arlandini, C. 1997, *ApJ*, 478, 332
- Tylenda, R., Acker, A., & Stenholm, B. 1993, *A&AS*, 102, 595
- Vauclair, G., Moskalik, P., Pfeiffer, B., & et al. 2002, *A&A*, 381, 122
- Werner, K. 1992, in *LNP Vol. 401: The Atmospheres of Early-Type Stars*, 401, 273
- . 1996, *A&A*, 309, 861
- Werner, K., Deetjen, J. L., Dreizler, S., Rauch, T., & Kruk, J. W. 2003, in *IAU Symposium*, ed. S. Kwok, M. Dopita, & R. Sutherland, *ASP, IAU Symp.* 209, 169
- Werner, K., Dreizler, S., Heber, U., Rauch, T., Wisotzki, L., & Hagen, H.-J. 1995, *A&A*, 293, L75
- Werner, K., Hamann, W.-R., Heber, U., Napiwotzki, R., Rauch, T., & Wessolowski, U. 1992, *A&A*, 259, L69
- Werner, K. & Heber, U. 1991, *A&A*, 247, 476
- Werner, K., Heber, U., & Fleming, T. 1994, *A&A*, 284, 907
- Werner, K., Heber, U., & Hunger, K. 1991, *A&A*, 244, 437
- Werner, K. & Koesterke, L. 1992, in *LNP Vol. 401: The Atmospheres of Early-Type Stars*, 401, 288
- Werner, K. & Rauch, T. 1994, *A&A*, 284, L5
- Werner, K., Rauch, T., Barstow, M. A., & Kruk, J. W. 2004a, *A&A*, 421, 1169
- Werner, K., Rauch, T., & Kruk, J. W. 2005, *A&A*, 433, 641
- Werner, K., Rauch, T., Napiwotzki, R., Christlieb, N., Reimers, D., & Karl, C. A. 2004b, *A&A*, 424, 657
- Werner, K., Rauch, T., Reiff, E., Kruk, J. W., & Napiwotzki, R. 2004c, *A&A*, 427, 685
- Wesemael, F., Green, R. F., & Liebert, J. 1985, *ApJS*, 58, 379

Wood, P. R. & Faulkner, D. J. 1986, ApJ, 307,
659

Young, P. A., Meakin, C., Arnett, D., & Fryer,
C. L. 2005, ApJ Lett., 629, L101

Zahn, J.-P. 1991, A&A, 252, 191